AD NUMBER

AD394475

CLASSIFICATION CHANGES

TO: unclassified

FROM: confidential

LIMITATION CHANGES

TO:

Approved for public release, distribution unlimited

FROM:

Controlling DoD Office.

AUTHORITY

Office of Naval Research ltr dtd 19 April 2000; Same.

Deep Ocean Ambient Noise (U)

Arthur A. Barrios

December 1957

ARTEMIS

REPORT NUMBER 64

Columbia University
in the City of New York
HUDSON
LABORATORIES

Hudson Laboratories
of
Columbia University
Dobbs Ferry, New York 10522

ARTEMIS Report No. 64

DEEP OCEAN AMBIENT NOISE (U)

by

Arthur A. Barrios

CONFIDENTIAL

December 1967

This report consists of 156 pages.

Copy No. of 100 copies.

This work was supported by the Office of Naval Research under Contract Nonr-266(66). In addition to security requirements which apply to this document and must be met, each transmittal outside the Department of Defense must have prior approval of the Office of Naval Research, Code 480.

ABSTRACT

The objective of this report is to provide information on deep ocean ambient noise which can be used in sonar system design and analysis. Guidelines are given for estimating wind-generated noise, oceanic ship traffic noise, biological noise levels, and the composite ambient noise background. The report also discusses recent measurements and studies on the directional properties of noise, and on the space-time correlations.

Early and recent reports on ambient ocean noise are reviewed and evaluated. Some conclusions are drawn on the variability of reported noise levels in the northwest Atlantic area and on the correlation of wind speed with respect to noise.

TABLE OF CONTENTS

LIST OF ILLUSTRATIONS AND TABLES IN TEXT

* Number identifies the reference to the paper from which this figure is reproduced.

LIST OF ILLUSTRATIONS AND TABLES IN APPENDICES

SUMMARY AND CONCLUSIONS

Summary

This report is a compilation of deep ocean ambient noise information. Its purpose is to serve as a reference source of ambient noise that can be used in sonar system design analysis and experimental planning. It also provides a set of guidelines for making rough estimates of ambient noise levels in deep ocean areas where experimental data is incomplete.

A set of guidelines* for estimating noise is constructed for prediction of wind generated noise, oceanic traffic noise, biological noise levels and the composite ambient noise background. The composite noise level due to various sources is obtained by adding the noise levels before conversion to decibels.

The respective noise levels may be estimated in the following steps:

1. Estimate wind-generated noise by using the oceanographic atlas charts.[18] This method was developed by the writer in the course of this noise study. The manner in which the wind speed data are obtained and analyzed is described using wind speed charts, wind speed data tabulations, and probability distributions of wind speeds.

2. Estimate oceanic traffic noise; some typical reports which provide one set of data on the density of ships in data on ships are by C. R. Rumpel,[40] Wenz,[19] and Weigle and Perrone.[6]

3. Estimate peak biological noise levels with respect to day, month, season, etc. from literature on density and distribution of marine life.[23,24] Determine when the biological noise peak effectively overrides other noise and blanks out the receiver.

* Guidelines for estimating noise have also been developed by others. Reference 28 refers to guidelines used in estimating noise levels; however, the basic guidelines do not appear in the referenced reports.

In the past decade, increasing attention has been directed to other characteristics of underwater noise. Measurements and studies have been performed on the directional properties of noise, and on the space-time correlations. Two current studies of interest are by R. J. Urick,[34] and E. M. Arase and T. Arase.[14] In his paper Urick hypothesizes two different noise types in a "mix" that depends on sea state and frequency. E. M. and T. Arase interpret ambient-noise correlograms in terms of sea-surface noise radiated with an intensity proportional to $\cos^n \alpha$. Some values of $n = 0 , 1/2 , 1 , 2$ were examined for different ranges of sea state and frequency. It was found at 250 Hz and sea state 5 that the data fit the $\cos^{1/2} \alpha$ model; at 400 Hz and above, for sea state 5, they found that a uniform distribtuion of $\cos \alpha$ radiators gives a good fit for spatial and principal peak of space-time correlations. At 400 to 1130 Hz, for sea state 3, they could not get any satisfactory fits to the theoretical model; a possible explanation, advanced here, is that at the receiver, for this sea state and frequency range, the magnitudes are the same order for the oceanic traffic noise and the sea-state noise.

The statistics of ambient noise are discussed in an internal Hudson Laboratories report by E. M. and T. Arase.[11] In their study they discuss the ambient noise statistical properties measured with an array of 30 to 60 elements. Although the noise distributions appear to be grossly normal, they show by means of the Kolmogorov-Smirnov tests that in general the distributions were nonstationary.

Conclusions

1. Yearly noise median.

There is no significant difference in the Artemis-Bermuda area among the yearly median noise levels reported by BTL (1962)[28] for the northwest Atlantic area, E. M. Arase and T. Arase (1966),[14] Weigle and Perrone (1966),[6] and Hasse (1966).[22] The difference in median noise levels between any two researchers rarely exceeded 4 dB.

2. Seasonal medians.

Winter season noise level medians in the Artemis area are not in close agreement. From Hasse[22] the winter season average noise level is -28 dB, while Arase[8] gives -34 dB. No explanation is available for the difference; it remains to be resolved. (C)

Summer noise levels in the same area (Artemis) agree closely; the differences among Hasse, Arase, etc. are not more than 2 dB.

3. Correlation of wind speed and noise.

In the Artemis area it was shown[6,8] that the wind speeds and wind-generated waves correlate very well (80 to 95 percent) with measured noise levels. Where similar close correlation between wind speed, waves and noise levels holds in other ocean areas, it is possible to use wind speed data (Oceanographic Atlas) to estimate monthly, seasonal, and yearly noise levels for the frequencies at which wind-generated noise is dominant. But, one must be careful in using the wind estimation technique. Wind speed by itself is a rough measure of noise; needed also are data on the "fetch" and duration of the wind.* An example of this is the Arases' report[9] in which a 5-dB difference is shown for the same wind speed in winter and in summer; the probable reason is that wind speeds in the winter season had a greater

* For a tutorial paper on "Wave Forecasting" see C. L. Bretschneider[33] paper.

"fetch" and duration than in the summer season. Therefore, when estimating noise levels from wind speeds a weighting factor corresponding to the season should be used. This weighting factor is related to the "fetch" and duration of the wind, and the generation of waves.

4. Oceanic traffic noise.

ppears from the literature that it is difficult to take the observed data and separate oceanic traffic noise from wind-generated noise. Some reports[28,6] attempt to do this, but it is not at all clear how it is done. The oceanic traffic noise estimates are based on studies of oceanic shipping patterns; in one case Wenz[19] admits an uncertainty factor spread of 10 dB in estimating the noise generated by a single ship.

This uncertainty factor is additive when summing up the total noise source contributions from a number of ship noise sources.

5. Directivity and space-time correlation.

The Artemis measurements indicate that the ambient noise field is anisotropic. The noise field directivity has a time variability; it is also a function of frequency, wind speed and ocean shipping distributions. An effective directivity index is usually used in analyzing system performance. This effective directivity is defined to be the signal-to-noise gain of the module relative to that of the reference omnidirectional hydrophone.

INTRODUCTION

Ambient noise is but a part of the overall background noise in a sonar surveillance system. The overall background noise comprises the following:

1. Ambient noise that is a property of the medium itself.
2. Self noise caused by the equipment and/or platform and noise* due to water currents about the hydrophones and movements of the hydrophones.
3. Reverberation noise that refers to unwanted returns due to active sonar backscattering from myriad scatterers in the ocean.

This report discusses only deep ocean ambient noise. The subjects of self noise and reverberation will be treated separately in subsequent reports.

The first comprehensive survey of ambient noise data was made during World War II by Knudsen et al.[1] in which ambient noise was correlated above 200 Hz with sea state and/or wind force. These average curves became standard for all underwater sound calculations until 1952. About that time researchers at Hudson Laboratories,[2,3] NEL,[4] and Bell Telephone Laboratories[5] noted that ambient noise levels below 300 Hz, 200 Hz, and 100 Hz often fall below the Knudsen curves and do not correlate well with the sea state. It was suggested that distant oceanic shipping would account for the low-frequency ambient noise. Re-examination of existing data shows that ambient noise spectra in the deep ocean could be described in terms of two overlapping spectra:

* This noise is sometimes considered as part of the "ambient" noise of the medium; it is not so in the true sense of the word. However, it is very difficult (if not impossible) to separate this type of self noise from the ambient.

1. a medium frequency spectrum (10 to 500 Hz) attributable to distant shipping,
2. a high frequency spectrum (20 Hz to 2 kHz) dependent on state of the sea.

Since 1954, the results of a large number of ambient noise measurements have added substance to the concept of the ambient noise spectra in the deep ocean. Also, studies of directivity, fluctuations, and correlations have added other dimensions to the ambient noise picture.

Since March 1963 a continuing ambient noise measurement program has been carried out by resident personnel at the USL, Bermuda Research Detachment. F. G. Weigle and A. J. Perrone in their latest report[6] give the results of a 23-month study of the noise spectra observed with three types of Artemis receivers, the three receiver types being an omnidirectional hydrophone, a down beam array, and an up beam array. A common feature noted from three sets of corresponding curves was that the observed levels were more subject to changes in wind speed at the higher frequencies than at the lower frequencies (i.e., below 178 Hz). E. M. Arase and T. Arase, of Hudson Laboratories, from 1963 on, have carried out a continuing program of Artemis ambient noise research studies. Their work has covered ambient noise spectra, sea state and wind dependence, and correlation of wind and noise,[7-10] and has been mainly concerned with noise statistics[11] and the directional properties and space time correlations of ambient noise.[8-10, 12-17] The results are important in predicting the performance of Artemis type sonar arrays in nonisotropic noise fields.

A method for estimating wind-generated noise by use of the Oceanographic Atlas Chart[18] is developed and discussed. The ambient noise levels derived from the estimated wind level agree reasonably well with the actual noise measurement median levels in the Artemis Bermuda area. This holds fairly well for frequencies (100 Hz to 1000 kHz) at which wind-generated noise is dominant. Since wind speed by itself provides only the basis for a rough estimate of noise, data on "fetch" and duration of the wind are also needed.

This report describes and collates much of the significant ambient noise research carried out to date. Attention is focused on deep ocean ambient noise sources, spectral characteristics, wind noise, oceanic traffic noise, biological noise, statistical characteristics and directional properties. It provides a set of guidelines for estimating ambient noise levels in a deep ocean area.

SOURCES OF AMBIENT OCEAN NOISE

Table I lists the sources of ambient noise along with the frequency band, spectrum slope, dependence, cause, and maximum level. The principal sources of interest to this study are oceanic ship traffic, hydrodynamic,* and biological.

1. Oceanic Traffic Noise

Traffic noise characteristics are determined by the mutual effect of three factors: transmission loss, number of ships, and the distribution of ships. The noise characteristics also depend on the nature of the source; however, the base is usually broad so that individual source differences blend into an average source characteristic. Wenz[19] in his review of surface ship noises indicates that the average sound-pressure-level spectra have a slope of about -6 dB per octave The spectrum is highly variable at frequencies below 1000 Hz; under certain circumstances the slope tends to flatten in the neighborhood of 100 Hz. This source-spectrum shape is altered in transmission by the frequency dependent attenuation part of the transmission loss. Variations in the spectra of the composite set of curves are said to be caused by differences in source depth, differences in the shape of the source-noise spectrum, and differences in the attenuation at different ranges.

It is known from long-range transmission experiments in deep water that propagation losses do not fit the free field spherical divergence law too well; better agreement with experiment does result if boundaries and sound velocity structure are taken into account.

---

* Includes wind-wave, rain, and various weather effects.

Table I

Sources of Underwater Ambient Noise

	Frequency Band	Spectrum Slope per Octave	Dependence	Cause	Maximum	Comments
(a) Thermal Noise	> 20 kHz	+ 6 dB	Thermal agitation. At temperatures between 0° and 30° C the thermal loss level is given by: $L_t = 10i + 20 \log f$ (in dB //.0002 dyne/cm^2)	Thermal agitation of the medium.	Increases with frequency.	Not significant below 10 kHz.
(b) Oceanic Ship Traffic	10 Hz - 1000 Hz	-6 dB	Density and distribution of traffic. Transmission loss.	Ship's machinery, flow noise.	20 Hz - 200 Hz	Effective distance can be as much as 1000 miles or more.
(c) Ship Noise	"	"	Proximity and number of ships to transducer.	Same as above	"	Usually obvious and can be deleted from noise data.
(d) Hydrodynamic	50 Hz - 10 kHz	-6 dB or -5 dB (above 1 kHz)	Sea state - Wind force and duration - Precipitation.	Bubbles, water droplets, surface waves, turbulence.	100 Hz - 1000 Hz	"Hydrodynamic" includes wind, wave, and other weather effects.
(e) Biological	10 Hz - 100 kHz		Frequency, time and location.	Shrimps, whales, fish etc.		Continuous noise encountered in some areas. Diurnal and seasonal patterns.
(f) Seismic	1 - 100 Hz		Highly dependent on time and location. It is usually a single transient of relatively short duration. However, in some areas may occur several times in one hour.	Volcanic and earthquakes.	2 - 20 Hz	May have direct effect on bottom-mounted transducers. Must take into account the vibration sensitivities of transducers.

UNCLASSIFIED

Table I (continued)

Sources of Underwater Ambient Noise

	Frequency Band	Spectrum Slope per Octave	Dependence	Cause	Maximum	Comments
(g) Explosions	Wide range		Magnitude of explosion.		Below 100 Hz	Characteristics very much like that of seismic.
(h) Precipitation	100 - 500 Hz		Magnitude and duration of precipitation.	Rain, hail.	Above 500 Hz	Noticeable for low wind speeds. See (d).
(i) Industrial activity				Pile driving, hammering, etc.		May predominate in near-shore areas.
(j) Sea - Ice	Wide range			Straining and cracking of ice, etc.		

Wenz[19] estimates 105 dB as the average transmission loss at 100 Hz for a range of 500 miles. At a range of 1000 miles the propagation loss would be 3 to 6 dB more. The source pressure levels for an average surface ship in a 1 Hz band at 100 Hz at one yard distances are assumed to be between 51 dB and 71 dB (relative to 1 μbar) in most instances. Therefore, the spectrum level (relative to 1 μbar) at 100 Hz from one average ship source is -54 dB to -34 dB; assuming power addition, the spectrum level at a distance of 500 miles, from 10 ships, would be -44 dB to -24 dB. From 100 ships the spectrum level would be -34 dB to -14 dB. Note that the effective distance for traffic-noise sources in the deep ocean can be as much as 1000 miles or more. The conclusion drawn by Wenz is that the nonwind-dependent component of the ambient noise at frequencies between 10 Hz and 1000 Hz is traffic noise. While many places are isolated from traffic noise, in a large part of the ocean traffic noise is a significant element of the observed ambient noise and often dominates the spectra between 20 Hz and 200 Hz.

In the Bermuda area Weigle and Perrone[6] have considered traffic noise as the most likely source of background noise seen by the Artemis receivers at frequencies below 178 Hz. They point out that the observed noise below that frequency is practically nonwind dependent and is relatively stable over long periods of time. The results of two studies of ship traffic density that were pertinent to the Artemis sector of interest are shown again in Table XI in the section on "Prediction of Ocean Traffic Noise."

2. Hydrodynamic Sources of Ambient Noise

Ambient noise is often produced by a wide variety of hydrodynamic processes. These processes are continually taking place, even at zero sea state. The main processes are due to water motion including the effects of surf, rain, hail, and tides. The various hydrodynamic processes are discussed further:

a. Bubbles and Cavitation

It is believed (Wenz[19]), that air bubbles and cavitation produced at or near the surface of the oceans, as a result of the action of the wind, are the main sources of wind-dependent ambient noise at frequencies between 50 Hz and 10 kHz. Both the level and shape of the observed wind-dependent ambient noise can be explained by the characteristics of bubble and cavitation noise.

Although the wind is the most important generating mechanism, bubbles are present in the ocean even when the wind speed is below that at which white caps are produced. The breaking of waves is not the only process which creates bubbles; they are also created by decaying matter, fish belchings, and gas seepage from the sea floor. There is also evidence of the existence of invisible microbubbles in the sea and of the occurrence of gas supersaturation of varying degree near the surface. These microbubble nuclei grow into visible bubbles as a result of temperature increases, pressure decreases, and turbulence associated with surface waves. As the bubles rise to the surface, they grow in size and are subjected to transient pressures; this induces the oscillations that generate the noise. On relatively quiet days, when there is no wind, bubbles have been seen to

emerge from below the water surface, sometimes persisting for a time as foam, and then to burst at the surface. At sea state zero, therefore, it is possible that nonwind dependent bubbles are significant contributors to underwater ambient noise. However, the surface agitation resulting from wind effects is the important process which produces an effective, highly efficient noise sound source in the form of oscillating bubbles.

Exact predictions of bubble noise in the ocean cannot be made because of insufficient observational data. However, some rough appraisals[19,20] have been made on the radiation of sound by air bubbles in the water. The natural frequency of oscillation for the zero mode is

$$f_o = (3\gamma p_s \rho^{-1})^{1/2} (2\pi R_o)^{-1} \qquad (1)$$

where γ is the ratio of specific heats for the gas in the bubble, p_s is the static pressure, ρ is the density of the liquid (ocean water), and R_o is the mean radius of the bubble. The amplitude of the radiated sound pressure at a distance d from the center of the bubble is

$$p_o = 3\gamma p_s r_o d^{-1} \qquad (2)$$

where r_o is the amplitude of the zero mode of oscillation. The zero mode refers to single volume pulsations. Only the zero oscillation mode is considered here because energy in the higher orders of free oscillation of the bubbles is negligible. Furthermore, in the case of forced oscillations, the sound energy tends to be concentrated at the natural frequency of oscillations of the zero mode; in some instances, however, the frequencies associated with the environmental fluctuations may be below the natural frequency of bubble oscillation.

The natural frequency is inversely proportional to the bubble size, and the radiated sound pressure amplitude is directly proportional to the bubble-oscillation amplitude. In general, it is expected that the spectrum has a maximum associated with either a predominant bubble size or a maximum bubble size; the exact shape of the spectrum will depend on the distribution of bubble sizes and of amplitudes of oscillation.

Using Eqs. (1) and (2), it was found that a spherical air bubble of mean radius 0.33 cm in water at atmospheric pressure, oscillating with an amplitude of 1/10 the mean radius ($r_o = 0.1\ R_o$), has a simple source pressure level at 1 m of about 59 dB above 1 μbar at a frequency of about 1000 Hz.[19] For a frequency of 500 Hz, the mean bubble radius is about 0.66 cm, and, for the same amplitude-to-size ratio, the source level is 6 dB higher.

The maxima in the observed wind-dependent ambient spectra occur at frequencies between 300 Hz and 1000 Hz; this corresponds to bubble sizes of 1.1 to 1.33 cm in mean radius. This is a reasonable order of magnitude. The characteristic broadness of the maxima in the wind-dependent ambient noise spectra can be explained if one assumes that in the surface agitation the bubble size and energy distributions are not sharply concentrated around the averages. The ambient noise high-frequency slope (-6 dB per octave) above the maximum value agrees with that of the bubble noise.

The shape of the spectrum* of wind-produced cavitation noise[21] is similar to that of air bubble noise. The amplitude of oscillation due to

* See Fig. 26 for curves of wind-generated noise spectrum.

cavitation is usually greater. This results in higher noise levels for vapor cavities than from the simple volume pulsations of gas bubbles. Cavitation is produced at or near the surface as a result of the action by the wind; it increases in intensity with the increase in wind-wave agitation

It may be concluded on the basis of the current evidence that air bubbles and cavitation produced at or near the surface are the main source of the wind-dependent ambient noise at frequencies between 50 Hz and 10 kHz.

b. Water Droplets and Precipitation

A spray of water at the surface of the sea will cause radiation of underwater noise. The noise is generated by the impact and passage of the droplet through the free surface. Moreover, air bubbles are usually trapped so that the total noise includes contribution from the bubble oscillations as well. The noise spectrum has a broad maximum near a frequency equal to twice the ratio of the impact velocity to the radius of the droplets. Toward low frequencies the spectrum decreases at a rate of 1 or 2 dB per octave. At frequencies above the maximum, the slope approaches -5 or -6 dB per octave. The impact part of the radiated sound energy increases with increase in droplet size and impact velocity. However, the relation is modified somewhat by the bubble noise, particularly at intermediate velocities.

Estimates[20] of noise spectrum levels due to rain (see Fig. 1) indicate that rain exceeding a rate of 0.1 in./hour will raise the noise levels and flatten the spectrum at frequencies above 1000 Hz under sea-state 1 conditions. In many instances higher wind speeds occur simultaneously with the rain. The resultant noise level in these instances is predominantly due to

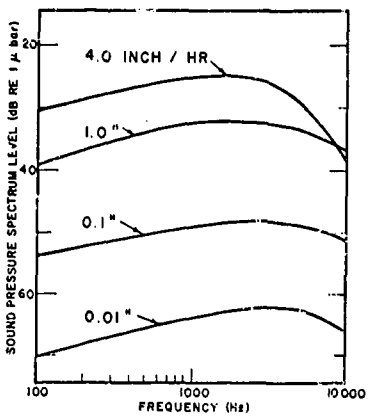

Fig. 1 Ambient noise spectrum level as estimated for rate of rainfall and frequency.

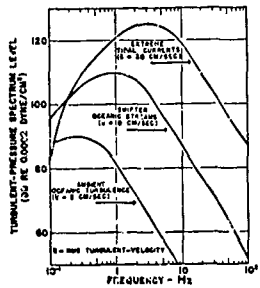

Fig. 2 Turbulent pressure level spectra.[19]

wind-dependent surface agitation rather than rain impact on the surface. At 400 Hz the increase in noise level due to rain has been observed to be about 2 dB over the same wind speed condition without rain.

c. Surface Waves (Subsurface Pressure Fluctuations)

A surface wave is a fluctuation in the elevation of the surface of a body of water; this causes subsurface pressure fluctuations. Wenz[19] indicates that the maximum of the energy spectrum occurs at frequencies below 0.5 Hz at wind speeds of Beaufort Force 3. As the wind speeds increase, the maximum noise energy level moves to lower frequencies. The effective frequency range of this noise source is well below 10 Hz.

d. Turbulence

Turbulence refers to the condition of unsteady flow with respect to both time and space coordinates.

Turbulence in the ocean occurs (1) at the ocean floor, particularly in coastal areas, straits, and harbors; (2) at the sea surface because of the movements and agitation of the surface; and (3) within the medium as a result of horizontal and vertical movements, such as advection, convection, and density currents. In his review, Wenz[19] concludes that noise radiated by turbulence does not greatly influence the ambient noise; but he indicates that turbulent pressure fluctuations are an important component of the noise below 10 Hz, and sometimes in the range from 10 to 100 Hz. Turbulent-pressure spectra derived by Wenz are shown in Fig. 2. The curve at the top shows the effect of extreme tidal currents.

e. Seismic Sources

A brief survey indicates that noise from earthquakes may be noticeable at frequencies between 1 Hz and 100 Hz; in general the spectrum has a

maximum between 2 and 20 Hz. However, such effects are transient and highly dependent on time and location. This suggests the possibility that some of the variability in ambient noise spectra in this frequency may be a consequence of seismic background activity.

It is conceivable that significant noise from lesser, but more or less continuous, seismic disturbances may be possible when ocean current velocities, turbulence, and oceanic traffic noise are at a minimum.

f. Biological Sources

Noise of biological origin covers a wide range of frequencies: 10 Hz to 100 kHz. Most of the noise energy from marine life is concentrated in the region between 100 Hz and 800 Hz. The contribution of biological noise to the ambient noise in the ocean varies with frequency, with time, and with location. Noise having the distinctive nature of biological sounds is often readily detected in the ambient noise; the biological source, however, is not always certain.

In some cases diurnal, seasonal, and geographical patterns may be predicted from experimental data, or from the habits and habitats of known noisemakers.

(C) Hasse[22] in a recent report indicates that in the Bermuda area biological noise has not, in general, been a problem to the Artemis system; however, at certain times and/or at certain receiver module locations, the effects of biological noise have been severe. Noise from whales is a seasonal problem, with the worst conditions persisting generally over the latter three to four weeks in April. The greatest whale noise occurs from dusk to dawn during the period of whale activity. Observations made in

a 12-hour period (15-16 April 1964) during a period of whale activity indicated that the receiver was whale-noise limited at 446 Hz for 77% of the time. Whale-noise to sea-noise ratios ranged to a maximum of 27 dB with ratios of 8 dB being the most frequent. This is shown in Fig. 3 along with three other frequency bands. The band centered at 224 Hz is the most affected of the four frequency bands; it is whale-noise limited 80% of the time. (C)

From publications showing the distributions of sharks and whales throughout the North Atlantic Ocean, it appears that the Bermuda area is the sparsest (marine life) populated in the North Atlantic.[23-26] From these references it would seem that biological noise sources could be significant and serious to the ambient noise background in the frequency region below 1 kHz.

In conclusion, when determining the ambient noise background for a particular area of ocean, it is important to estimate the magnitude, location, and other characteristics of the biological noise sources.

g. Sonic Boom Sources

The introduction of the Super Sonic Transport (SST) into commercial air service in the 1975 era may result in a new source of underwater ambient noise in some ocean areas. Shock waves are a normal consequence of supersonic flight in the atmosphere; they pass over the ground and ocean surface and result in excess pressures of 1 to 3 pounds per square foot (psf). As the shock wave travels over the ocean surface, a certain amount of the energy will be transformed into underwater noise.

It is not possible at this time to assess the magnitude and other characteristics of the underwater noise generated by the sonic boom. The

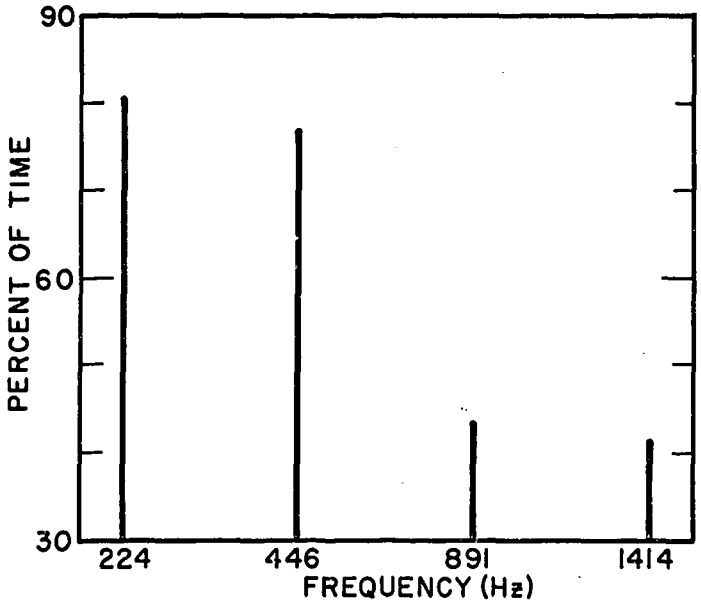

Fig. 3 Percent of time whale-noise limiting occurred in four logit bands. Measurements during a 12-hour period, April 15-April 16, 1964.[22]

manner in which the sonic boom energy may be transformed into underwater noise is not clearly understood at this time.* One possible mode of energy transformation may involve the refraction of the incident sonic boom ray, at the ocean surface, into the water. Another possible mode of energy transformation may involve the cavitation (and subsequent noise) induced by the negative pressure points in the sonic boom "N" wave; this cavitation process might be enhanced by the usual presence of bubbles just below the ocean surface.

* A more detailed description and discussion on the sonic boom noise source is contained in Hudson Laboratories Technical Memorandum No. 85, On the Sonic Boom Generation of Ocean Noise, by A. Barrios.

AMBIENT NOISE SPECTRUM COMPONENTS

A simplified model of the ambient noise spectrum, by Wenz[19] resolves the spectrum between 1 Hz and 10 kHz into several overlapping subspectra (see Table II). Although the effects of marine life, nearby ships, explosions, industrial activity, etc. are not included, the Wenz model provides a good starting point for understanding the complexities of underwater ambient noise. Later one may add to the basic model the effects of marine life and of any other additional sources that may be significant contributors in a particular location and time.

The basic ambient noise spectrum model is resolved into three overlapping subspectra:

1. Ambient Turbulence Spectrum

This is a low-frequency spectrum with a -8 dB to -10 dB per octave spectrum level slope in the range of 1 Hz to 100 Hz. A comparison of low-frequency noise measurements made in five different areas by Wenz[19] indicates that the noise level may differ by 20 to 25 dB from one place to another and from one time to another. The -8 dB to -10 dB spectrum slope may not always be true. Between 10 Hz and 100 Hz the spectrum may sometimes flatten and may even show a broad maximum; however, in other instances the spectrum slope shows little or no change from the slope below 10 Hz.

2. Nonwind-Dependent Spectrum

The nonwind-dependent spectrum is in the range of 10 Hz to 1000 Hz. The maximum level is between 20 to 100 Hz. Above 100 Hz it ordinarily,

Table II

Principal Components of Prevailing Ambient Noise in Deep Ocean[1]

Spectra	Frequency Band	Spectrum Level Slope per Octave	Source	Maximum	Additional Remarks
(a) Ambient Turbulence	1 Hz - 100 Hz	-10 dB	Ambient turbulent pressure fluctuations due to seismic activity, explosions, surface waves.	Sometimes at 10 Hz to 100 Hz	Nearly always predominant below 10 Hz; however influence sometimes evident up to 100 Hz in absence of nonwind-dependent and wind-dependent components.
(b) Nonwind-Dependent	10 Hz - 1000 Hz	-6 dB	Most probable source is oceanic traffic.	20 Hz - 200 Hz	Traffic noise makes up greater part of nonwind-dependent component of ambient noise. May be still significant at 400 Hz for sea states below SS4. Frequently predominates in band from 20 Hz to 200 Hz but is not observed in isolated ocean areas.
(c) Wind-Dependent	50 Hz - 10 kHz	-6 dB	Bubbles and spray from surface agitation due to wind.	100 Hz - 1000 Hz	Nearly always predominates above 500 Hz.

but not always, falls off rapidly. The most probable source is oceanic traffic.

3. Wind-Dependent Spectrum

The wind-dependent spectrum is in the range of 50 Hz to 10 kHz with a broad maximum between 100 Hz and 1000 Hz; above 1000 Hz, the spectrum slope is -5 dB or -6 dB per octave. Above 500 Hz the effects of wind-generated ambient noise always prevail. The most probable source is bubbles and spray due to surface agitation by the wind.

SURVEY OF AMBIENT NOISE RESEARCH

A continuing program of ambient noise measurements has been carried out as a part of the Artemis research studies. The Artemis investigations of ambient noise have used two approaches. One has been the long-term measurements consisting of automatic broad-band recording of the outputs of many sensors, providing two-minute noise samples on magnetic tape every two hours; the other approach has involved short-term measurements consisting of continuous recordings of the filtered outputs of one or more selected sensors for periods of hours or days made at irregular intervals in pursuit of specific points of interest. Correlative environmental data in the form of wind speed and direction and wave height have been recorded for both long- and short-term measurements. The long-term measurements have to date extended over a two-year period and cover ten contiguous logit frequency bands in the interval of 100 to 1000 Hz. (C)

1. USNUSL Artemis Noise Measurements

The latest available report is (dated Dec. 1966) "Ambient Noise Spectra in the Artemis Receiver Area," by F. G. Weigle and A. J. Perone.[6] Results are presented of a 23-month study of the noise spectra observed with three types of Artemis receivers of Bermuda. The data were grouped in 10 wind speed intervals between zero and 50 knots and examined at 10 logit frequencies between 112 Hz and 891 Hz. Curves of spectrum levels versus frequency are shown for an omnidirectional hydrophone (Fig. 4), an up beam array (Fig. 5), and a down beam hydrophone array (Fig. 6). A common feature noted from the three sets of curves is that the observed levels are more subject to changes in wind speed at the higher frequencies than at the lower frequencies. (C)

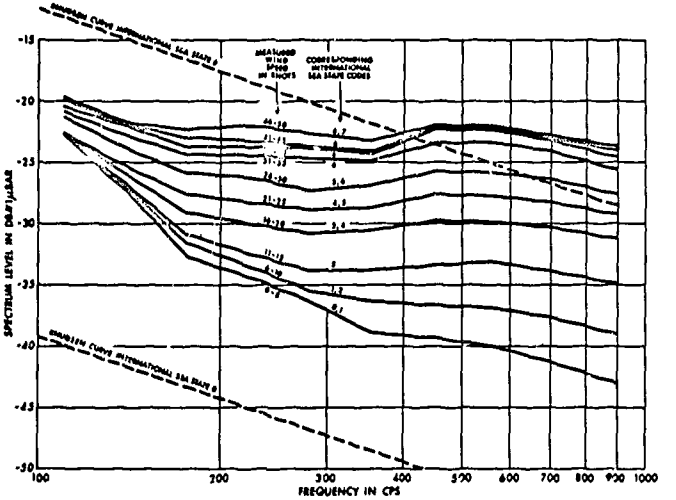

Fig. 4 Ambient noise spectra at the Artemis omnidirectional hydrophone.[6]

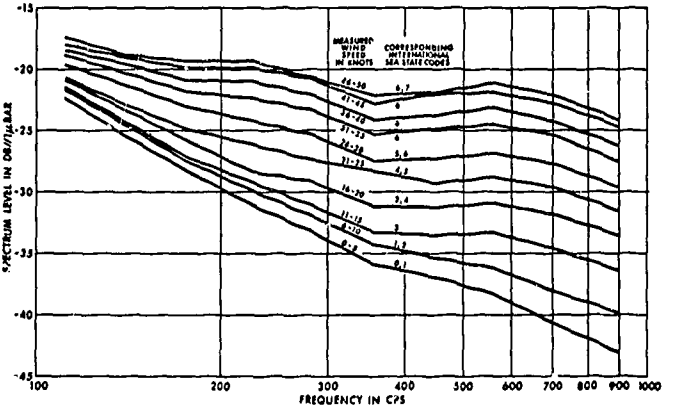

Fig. 5 Ambient noise spectra at the Artemis array up-beam module.[6]

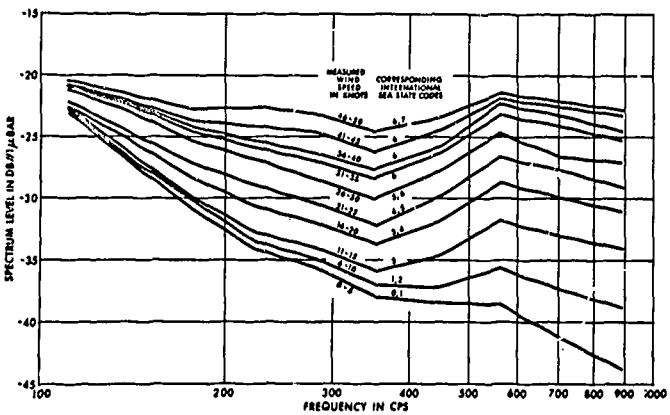

Fig. 6 Ambient noise spectra at the Artemis array down-beam module.[6]

A comparison of the spectra in Figs.4, 5, and 6 indicates that the shapes are quite similar in all cases. Corresponding levels differ by 4 dB at the most and generally fall within a 2-dB spread among the three receivers.

Greatest deviation occurs between the omnidirectional hydrophone and the up beam module at the lower frequencies (near 178 Hz) and at low wind speeds.* In this region the module outputs are relatively high, as might be expected from a consideration of the vertical pattern (Fig. 7) of this module. It has been concluded that the observed noise at those frequencies originated as traffic noise at long ranges. Such signals would arrive at the Artemis receiving array as low angle arrivals centered around 13° from the horizontal. The up beam module is, of course, designed to favor reception at an angle 13° above the horizontal and will tend to reject local surface noise more effectively than will the omnidirectional hydrophone; hence the up beam module will demonstrate a greater response to traffic-originated noise than will the reference hydrophone. (C)

The same argument can be applied to the down beam module. However, in this case the argument is modified to include the fact observed in past Artemis propagation measurements that some portions of the signal energy arriving along low-angle paths (below -13° from the horizontal) will actually reflect upward from the "knee" of the slope of Plantagenet Bank and be scattered away from the receiver. This may account for the fact that the received signal levels at the low frequencies are lower in the case of the down beam module than they are in the case the up beam module.

* Received signals at the low frequencies are much lower when the down beam module is used.

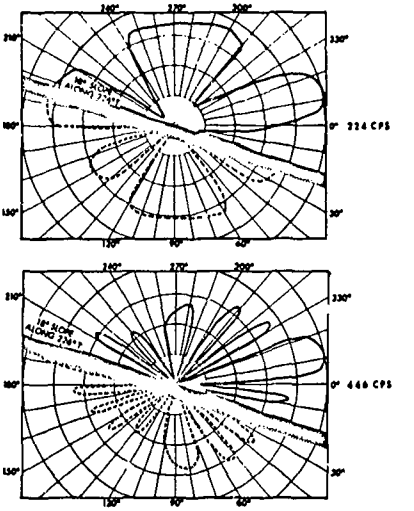

Fig. 7 Vertical patterns at 224 Hz and 446 Hz frequency of Artemis up-beam module.[6]

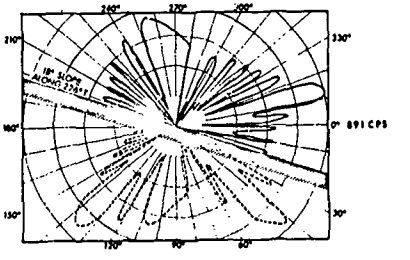

Fig. 8 Vertical patterns of 891 Hz frequency of Artemis down-beam module.[6]

Finally, the exaggeration of the peak at 562 Hz observed in the spectra for the down beam module (Fig. 6) is very likely associated with the strong upward-directed side lobes seen in the vertical pattern of the hydrophone receiver (Fig. 8) at the highest frequencies. (C)

The down beam module does not discriminate as effectively against local surface noise as does the up beam module, but neither does it show as high a response to low-frequency distant traffic noise.

A comparison of Artemis[6] data can be made with that reported by Walkinshaw[27] of BTL.* In Fig. 9 the median Artemis ambient noise spectrum for the case of the omnidirectional receiver is superimposed on the BTL curves of median ambient noise spectrum levels in the Northwestern Atlantic. The BTL median curve is a composite spectrum obtained from observations at many locations. The upper and lower curves observed at different locations are the respective limits of the individual median levels observed at the different locations. The shape correspondence between the Artemis curve and the BTL curve is generally good except at 891 Hz where the difference is 5 dB. (C)

Another ambient noise summary was reported by A. D. Little, Inc.[28] The portion of these idealized average ambient noise spectra comparable to the Artemis data reported here are reproduced in Fig. 10. The dashed curves respresent estimated noise due to shipping for a receiver in the Bermuda area. The solid-line curves represent sea-generated noise at the wind speeds indicated.

A composite of the idealized curves can be constructed by adding the power of the curve due to average shipping noise in the Bermuda area (Fig. 10)

* See Appendix B for comparison of Artemis data with data from other areas.

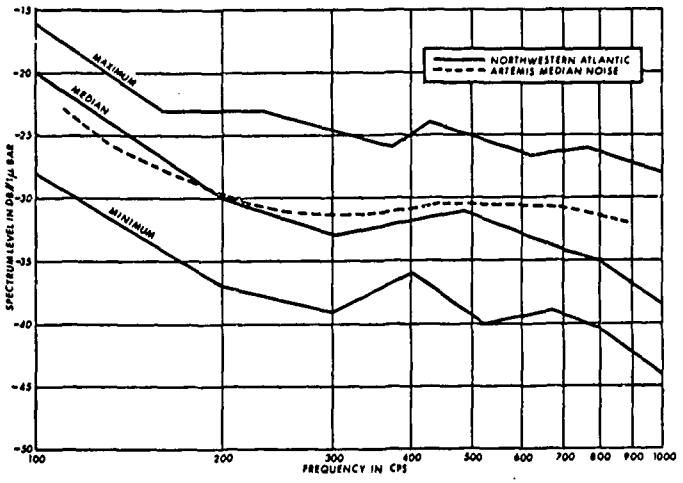

Fig. 9 BTL median ambient noise spectrum levels in Northwestern Atlantic.[6]

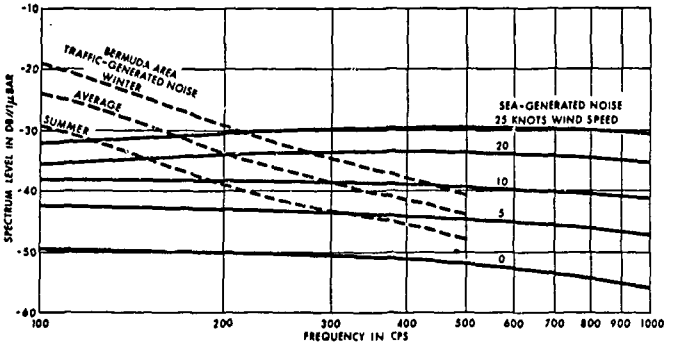

Fig. 10 A. D. Little idealized average spectra of ambient noise.[6]

with each one of the sea-generated wind-wave noise curves in turn. To accomplish this, a straight line extrapolation of the shipping noise curve between 500 Hz and 1000 Hz is assumed. In Fig. 11 the resulting composite spectra are shown and compared with the Artemis data from Fig. 4 at the four wind-speed intervals in closest correspondence. The Artemis data tend to predict a high ambient noise level with a maximum difference of about 5 dB at the highest frequencies. The two sets of data agree reasonably well in overall shape, supporting the prediction of ADL concerning the contribution of traffic noise at the low frequencies. The curve shape is also in reasonable accord with Wenz,[19] who attributes the spectrum from 50 Hz to 10,000 Hz to a wind mechanism with a broad maximum occurring between 100 Hz and 1000 Hz. (C)

A pattern common to all three wave types is apparent in the values of standard deviation plotted by Weigle and Perrone[6] in Fig. 12. This pattern does not appear to relate the standard deviation to sample size in general, but to other factors. In Fig. 12 the resultant standard deviations are plotted at each of ten wind-speed groups for four frequencies. The standard deviation at 446 Hz and 224 Hz increases as the wind speeds fall below 35 knots; the number of sample points increase as the winds drop from 35 to 6 knots. Above 35 knots the sample sizes are small and the deviations larger, as expected in such circumstances. At lower frequencies, the standard deviation becomes less dependent on wind speed, and at the lowest frequency (112 Hz) it is practically independent of wind speed. Finally, while the values of standard deviation demonstrate a dependence on frequency at low wind speeds (below 20 knots), no such frequency dependence is observed at higher wind speeds. It appears that the ambient noise

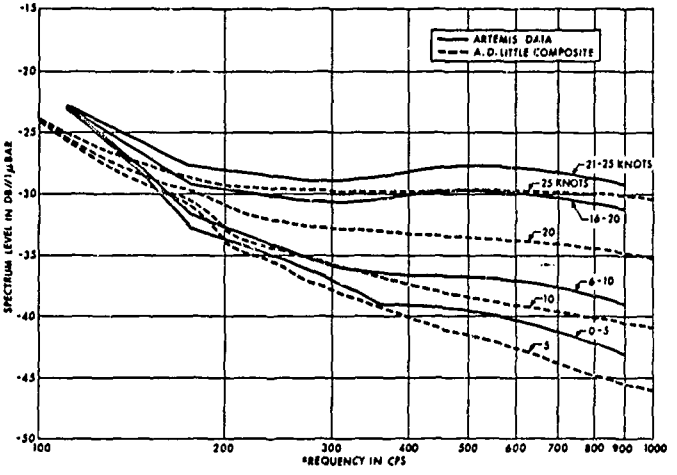

Fig. 11 Idealized co..iposite spectra of traffic and sea noise compared with Artemis spectra.[6]

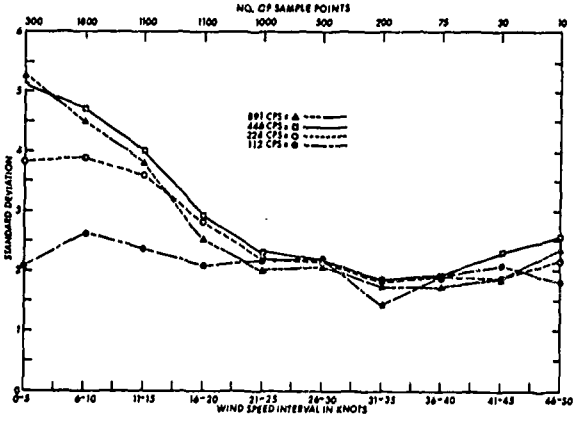

Fig. 12 Standard deviation vs. wind speed interval.[6]

levels at 112 Hz are much less dependent upon wind speed; the reason is that these low-frequency noise levels probably are largely the result of distant traffic noise at all wind speeds. (C)

2. Hudson Laboratories Artemis Noise Research

The Artemis ambient noise research at Hudson Laboratories has been conducted primarily by T. Arase and E. M. Arase. Table III indexes their work. Some of it has already been referred to in the present report. The reports and papers on ambient noise directional properties is referenced and discussed subsequently in another section.

The most recent work by Arase[11] deals with the statistics of ambient noise. Up to this time this subject had not been studied in connection with arrays, although ambient noise statistics were investigated previously for single receivers.[29] In the Arase report data are presented for ambient noise measured with arrays* of 30 to 60 receiver elements in the frequency range 300 Hz to 500 Hz. Amplitude samples of noise (2000 to 3000 samples) were taken at 30-msec intervals; this period was long enough to ensure that successive samples were independent. Samples were also taken at 1 to 3 msec intervals to obtain dependent sets of samples. Noise statistics were also taken with random addition of the elements.

Figure 13 shows the signal-to-noise ratio as a function of the number of elements. Figures 14 and 15 show the ambient noise (independent samples) cumulative distribution for random delays and for a steered array; ordinate values are the deflection in centimeters and deflection in volts. Figure 16 shows the noise cumulative distribution for three sets of dependent

* The arrays were steered for RSR arrivals.

Table III

Index of Reports and Papers by Subject -

Authored by T. Arase, E. Arase, et al.

Subject	References
Review of ambient noise	30, 31
Ambient noise records	7, 8
Spectra	7, 8, 9, 10
Sea state and wind dependence	7, 8, 9, 10
Correlation coefficient, wind and noise	7, 8
Precipitation	7
Ambient noise statistics	11
Directional Properties	
Space-Time correlations	12, 13, 10, 14, 5
Noise gain	15, 8, 9
Effective directivity index	8, 9
Signal/noise calculations	8
Noise models	15, 10
Arrays in noise fields	16, 17, 15, 32

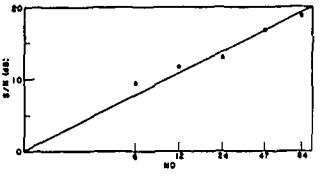

Fig. 13 Signal-to-noise ratio as a function of the number of elements.[11]

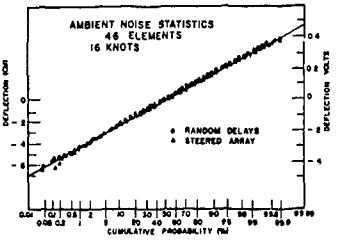

Fig. 14 Sets I and II.[11]

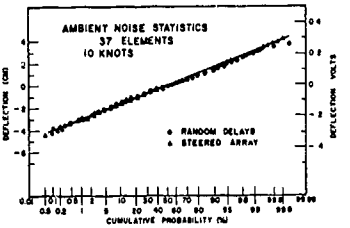

Fig. 15 Sets III and IV.[11]

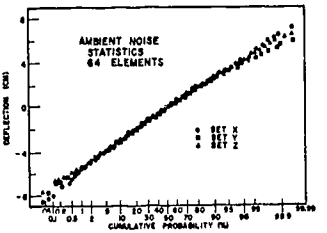

Fig. 16 Dependent sets X, Y, and Z.[11]

noise samples; these sets vary as much from each other as the steered and random delays do in the previous figures. Although the distributions appear to be broadly normal, Arase shows by means of the moment and Kolmogorov-Smirnov tests that sets III, IV, and X, Y, and Z exceed the 99% confidence interval for a Gaussian distribution; stationarity tests (using the Kolmogorov-Smirnov test) indicated that in general the distributions were nonstationary.

PREDICTION OF WIND-GENERATED NOISE

1. Prediction of Surface Winds

A. D. Little[40] indicates that Oceanographic Atlas charts have been used to estimate the mean ambient noise level generated by surface winds. However, the specific atlas and the method used is not explained in the referenced publication. In this report we have determined surface wind predictions from the Oceanographic Atlas charts[18] (for the North Atlantic). These charts provide information on the frequency distribution of surface winds in particular areas of the Atlantic Ocean. The frequency distributions are derived from data collected over a period of years at various observation areas. An example of one of the charts is shown in Fig. 17 "Surface Wind Roses, January." Charts for the other months of the year are also provided in the Atlas.

The coordinates for the Bermuda area are approximately 32° N, 63° W. The center of the nearest wind rose to the Bermuda area is 33° N, 67° W. At this wind rose location the cumulative probability distribution in percent is given in the form of a bar graph; this has been transformed in Fig. 18 to a cumulative frequency distribution of the wind speed for the month of January.* From this plot the mean wind speed appears to be 14 knots and the estimated standard deviation is 12 knots. The wind speeds used in the curve of Fig. 18 represent the top wind speed for the particular Beaufort number indicated in the bar graph of Fig. 17. For example: 16 knots is the top wind speed in Beaufort Force number 4; 16 knots then corresponds to the cumulative frequency of 59%.

* See Appendix A for wind speed distributions - February through December.

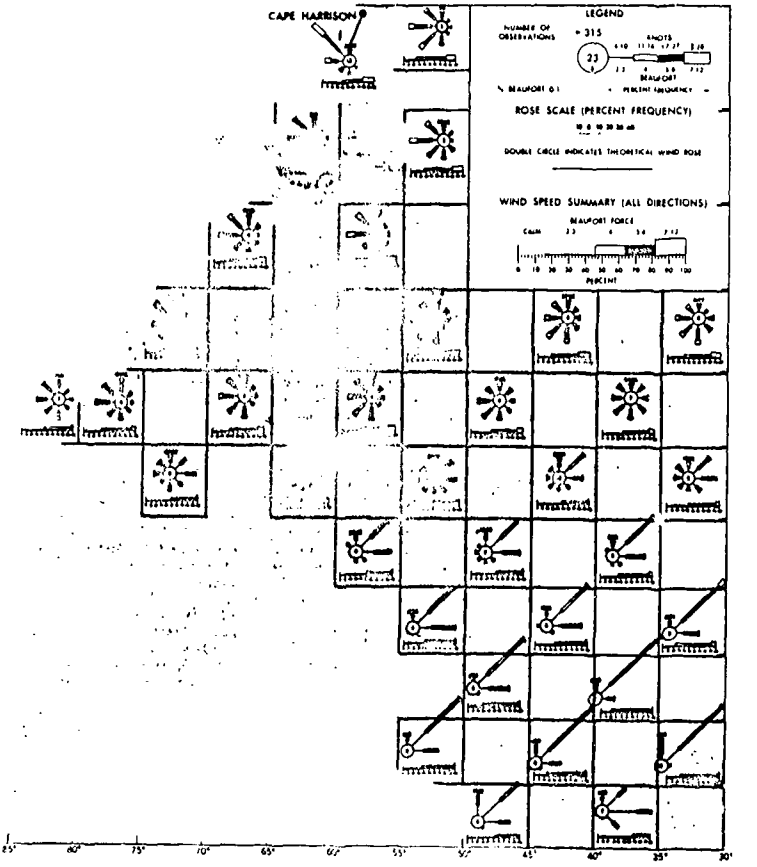

Fig. 17 Surface wind roses, January (from Oceanographic Atlas[18]).

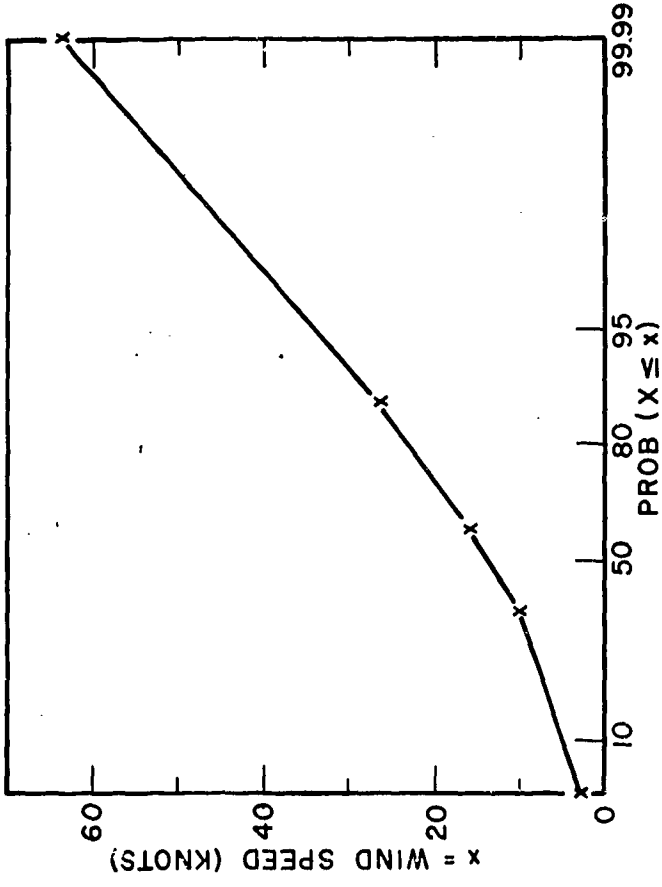

Fig. 18 Cumulative distribution of wind speeds for January.

Bar graph data on January and the other months of the year were obtained from the Oceanographic Atlas and tabulated in Table IV along with estimated yearly wind speed averages; the cumulative frequency distribution curve for the yearly median is shown in Fig. 19 with a mean wind speed of 11 knots and an estimated standard deviation of 12 knots. Also shown in Fig. 19 are three distribution curves[22] for Argus Island, Bermuda based on measured wind data for the years 1962, 1963, and 1964; the average mean wind speed for these three curves is 15 knots and the standard deviation is 9 knots. The reason for the difference between the Argus Island mean wind speed value (15 knots) and that of the estimated mean (11 knots) from the Oceanographic Atlas data is not immediately obvious and subject to some speculation. Some possible reasons are:

(1) The Argus Island wind speeds were constantly measured and recorded by the same instrumentation. On the other hand, the Oceanographic Atlas wind data were obtained by a variety of instruments and observers in the ocean area (Fig. 17) bounded by the coordinates 30° N to 35° N and 65° W to 70° W; the number of wind speed observations totals 30,000 samples. One would expect that instrumentation and observation errors would tend to average out in such a large and diversified sampling of data. It would appear reasonable to place greater credence on Oceanographic Atlas data than the data obtained by one instrument at one location. However, the fact that the Argus Island data are based on three years of measurements makes these data difficult to discredit.

(2) Another possible reason for the difference in the mean wind speed may lie in the use of the Beaufort wind force numbers. A Beaufort wind force number of, say 4, includes wind speeds of 11 to 16 knots; a Beaufort

Table IV Wind Speed Cumulative Frequency Distribution Data (Derived From Reference 18)
For Four Wind Roses at 33° N, 67° W; 27° N, 63° W; 37° N, 63° W; and 34° N, 57° W

(33° N, 67° W)		Jan	Feb	Mar	Apr	May	Jun	Jul	Aug	Sep	Oct	Nov	Dec
Number of Samples →		2660	2757	2856	2564	2434	2358	2549	2352	2536	2654	2487	2470
Beaufort No.	Wind Range 0-3 knots	5%	4%	5%	7%	12%	13%	13%	13%	13%	8%	6%	5%
2-3	4-10	36	32	36	44	58	65	66	61	60	44	41	35
4	11-16	59	53	60	68	83	87	88	85	81	70	64	57
5-6	17-27	87	85	90	96	100	100	100	98	97	96	93	87
7-12	28-64	100	100	100	100	-	-	-	-	100	100	100	100
(27° N, 63° W)													
Number of Samples →		1736	1802	2231	1873	1649	1572	1347	1230	1324	1356	1436	1650
Beaufort No.	Wind Range 0-3 knots	8%	8%	9%	12%	11%	19%	14%	16%	21%	10%	9%	10%
2-3	4-10	50	54	54	62	66	75	76	73	68	60	50	57
4	11-16	74	77	77	86	92	95	96	93	86	84	76	83
5-6	17-27	96	97	97	98	100	-	-	98	98	98	97	98
7-12	28-64	100	100	100	100	-	-	-	100	100	100	100	100
(37° N, 63° W)													
Number of Samples →		3491	3419	3893	4133	4739	4526	3711	3487	3267	3429	2265	3117
Beaufort No.	Wind Range 0-3 knots	3%	3%	3%	3%	6%	8%	9%	9%	7%	6%	5%	3%
2-3	4-10	21	18	19	29	38	43	46	51	43	36	28	22
4	11-16	38	36	37	51	62	68	72	75	67	46	50	38
5-6	17-27	73	70	74	85	92	97	96	96	94	90	82	74
7-12	28-64	100	100	100	100	100	100	100	100	100	100	100	100
(34° N, 57° W)													
Number of Samples →		2428	2623	3150	2441	2422	2257	2286	2179	2299	2205	2466	2643
Beaufort No.	Wind Range 0-3 knots	6%	4%	6%	10%	12%	14%	18%	20%	14%	11%	7%	5%
2-3	4-10	35	31	37	50	60	64	75	78	66	51	41	35
4	11-16	56	51	58	72	83	86	93	91	84	75	67	58
5-6	17-27	86	84	89	96	98	100	100	98	98	96	95	90
7-12	28-64	100	100	100	100	100	-	-	-	100	100	100	100

UNCLASSIFIED

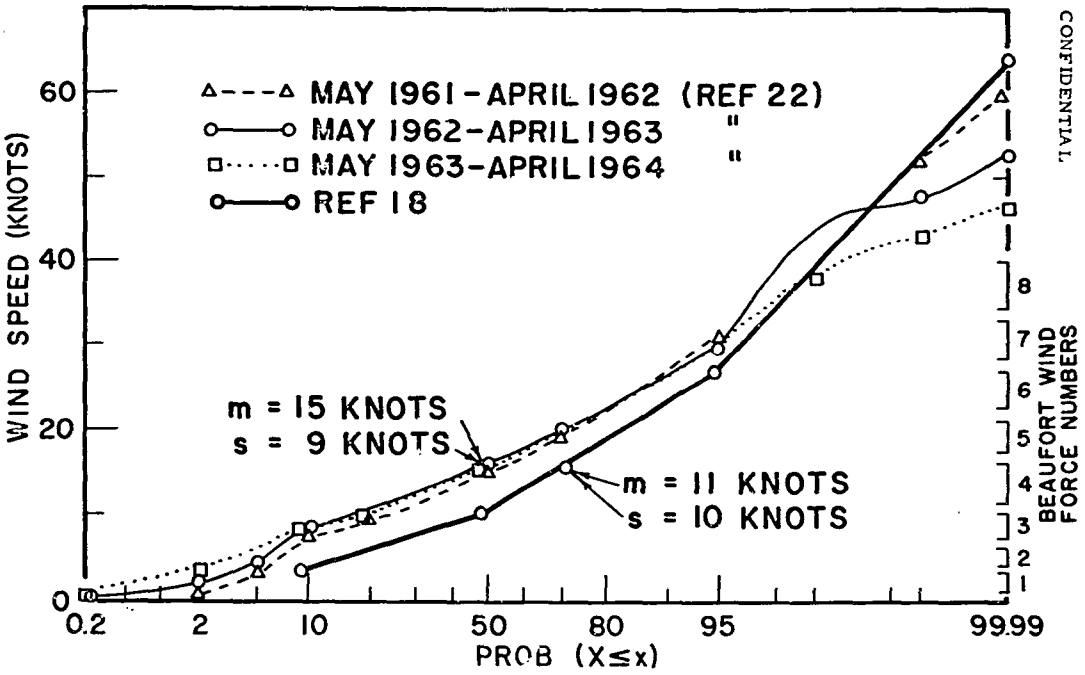

Fig. 19 Cumulative probability distribution data from Refs. 22 and 18.

number 3 includes wind speeds of 7 to 10 knots. It is possible that a large number of measured wind speeds tended to fall between 10 and 11 knots; these measurements might have been lumped in with the Beaufort number 3 (7 to 10 knots) and would skew the frequency distribution toward the lower Beaufort wind numbers; this in turn lowers the estimate of the near wind speed.

(3) A third possible reason is that the quadrangle bounded by coordinates 30° N to 35° N and 65° W to 70° W was not truly representative of wind speed conditions at the Bermuda coordinates of 32° N, 63° W. This hypothesis has been investigated by averaging in the wind rose data in the nearest three other quadrangles bounded by coordinates: 35° N to 40° N and 60° W to 65° W; 30° N to 35° N and 55° W to 60° W; 25° N to 30° N and 60° W to 65° W. The data derived from the respective wind rose bar graphs for all months of the year are tabulated in Tables V and VI along with the data of the quadrangle at 30° N to 35° N and 65° W to 70° W. Figure 20 is a distribution of the yearly median for the combined four sets of data. The total number of observations for distribution is over 120,000 sample points. Note that the mean wind speed value is now 11.5 knots and that the standard deviation is 16 knots (as compared with 12 knots previously). This result implies that the mean wind speed in the greater ocean area around Bermuda is still approximately 11 knots. However, one is again faced with the fact that the Argus Island wind data measurements indicate a yearly mean speed of 15 knots. The nearness of the Argus Island wind measuring instruments to the Bermuda land mass may be the cause: the effect of such a land mass is to increase the wind speeds in the area.

Table V

Tabulation of Cumulative Wind Speed Observations at the Four Wind Roses and Weighted Averages

(33° N, 67° W) Beaufort No.	Wind Range	Jan	Feb	Mar	Apr	May	Jun	Jul	Aug	Sep	Oct	Nov	Dec	Total	Weighted Average
0-1	0-3 knots	133	111	143	179	292	307	338	306	330	212	149	123	2,623	8.4
2-3	4-10	955	875	1030	1130	1410	1530	1720	1440	1520	1170	1020	863	14,663	47.6
4	11-16	1570	1460	1715	1740	2020	2050	2280	2000	2060	1850	1590	1405	21,740	70.7
5-6	17-27	2320	2540	2570	2460	2434	2358	2599	2310	2460	2540	2310	2140	29,041	94.6
7-12	28-64	2660	2757	2856	2564	-	-	-	2352	2536	2654	2487	2470	30,727	99.99
(27° N, 63° W)															
0-1	0-3 knots	139	144	201	224	181	298	188	197	278	136	129	165		
2-3	4-10	865	970	1200	1160	1090	1180	1020	900	900	814	715	940		
4	11-16	1280	1390	1715	1610	1520	1490	1290	1145	1140	1140	1090	1370		
5-6	17-27	1660	1750	2160	1830	1649	1572	1347	1210	1300	1330	1390	1620		
7-12	28-64	1736	1802	2231	1873	-	-	-	1230	1324	1356	1436	1650		
(37° N, 62° W)															
0-1	0-3 knots	105	103	117	124	284	348	354	314	229	206	113	94		
2-3	4-10	733	616	740	1200	1800	1830	1710	1780	1410	1235	634	687		
4	11-16	1330	1230	1440	2110	2940	2900	2670	2720	2190	1580	1130	1185		
5-6	17-27	2550	2400	2880	3510	4350	4130	3565	3350	3080	3090	1860	2300		
7-12	28-64	3491	3419	3893	4133	4739	4256	3711	3467	3267	3429	2265	3117		
(34° N, 57° W)															
0-1	0-3 knots	145	105	189	244	291	315	410	435	323	242	173	132		
2-3	4-10	846	814	1170	1220	1450	1440	1710	1530	1320	1120	1010	925		
4	11-16	1360	1340	1830	1760	2010	1940	2120	1980	1930	1650	1650	1530		
5-6	17-27	2080	2200	2810	2340	2370	2257	2286	2140	2270	2110	2340	2380		
7-12	28-64	2423	2623	3150	2441	2422	-	-	2179	2299	2205	2666	2643		
Weighted Averages for the Respective Months															
0-1	0-3 knots	5.07%	4.37%	5.37%	7.0%	9.3%	11.9%	12.9%	13.5%	12.3%	8.3%	6.5%	5.2%		
2-3	4-10	33.0	30.9	34.2	42.8	51.2	56.8	62.8	61.1	56.8	45.4	39.1	34.5		
4	11-16	53.8	51.1	55.3	65.6	75.4	78.4	84.6	84.6	77.6	65.1	63.1	55.6		
5-6	17-27	82.5	83.8	86.0	93.3	96.0	96.4	99	97.4	96.6	94.8	91.3	85.4		

UNCLASSIFIED

Table VI

Combined Weighted Cumulative Percentages for Four Wind Roses
at 33° N, 67° W; 27° N, 63° W; 37° N, 62° W; 34° N, 57° W

Beaufort No.	Wind Speed	Jan	Feb	Mar	Apr	May	Jun	Jul	Aug	Sep	Oct	Nov	Dec		
0-1	0-3 knots	5.07%	4.4%	5.4%	7.0%	9.3%	11.9%	12.9%	13.5%	12.3%	8.3%	6.5%	5.2%		
2-3	4-10	33.00	30.9	34.2	42.8	51.2	56.8	62.8	61.1	56.8	45.4	39.1	34.5		
4	11-16	53.8	51.1	55.3	65.6	75.4	78.4	84.6	84.6	77.6	65.1	63.1	55.6		
5-6	17-27	82.5	83.8	86.0	93.3	96.0	96.4	99.0	97.4	96.6	94.8	91.3	85.4		
7-12	28-64													Total	Weighted Average
0-1	0-3	524	465	654	776	1,040	1,275	1,275	1,250	1,160	784	562	514	10,279	8.4
2-3	4-10	3,400	3,270	4,140	4,750	5,730	6,080	6,200	5,650	5,350	4,340	3,380	3,410	55,700	45.4
4	11-16	5,550	5,410	6,700	7,280	8,440	8,380	8,750	7,840	7,300	6,210	5,450	5,500	82,420	67.2
5-6	17-27	8,500	8,870	10,140	10,400	10,750	10,300	9,800	9,000	9,100	9,050	7,850	8,430	101,790	83.0
7-12	28-64	10,315	10,601	12,130	11,011	11,244	10,716	9,893	9,248	9,426	9,554	8,654	9,880	122,673	99.9999

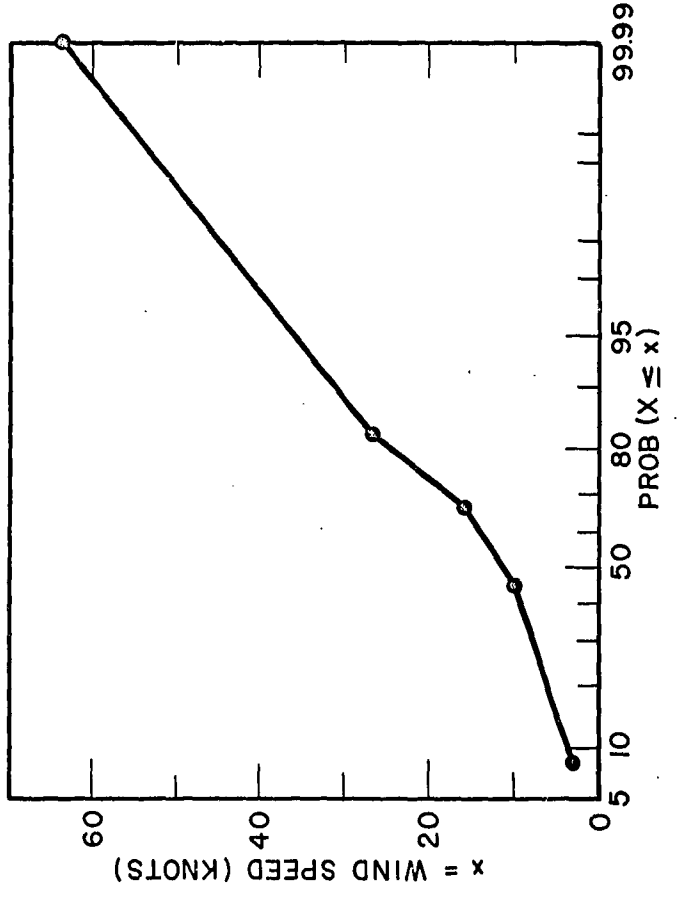

Fig. 20 Combined wind speed distributions (weighted).

(4) Finally we should note that the standard deviations are rather large with respect to the means. Therefore, the differences may be insignificant between the mean observed Argus wind speeds and the estimated Atlas wind speeds.

2. State of the Sea and Swell

Waves on the ocean surface are dependent primarily on the wind speeds. In the Oceanographic Atlas[18] the terms "sea" and "swell" describe the surface of the ocean. "Sea" refers to waves generated by local winds blowing over the water. These waves are short in period, closely approximate the direction of the generating wind when considered as a group, appear in combinations of various short crested heights, and give the semblance of a rapidly changing irregular surface.

"Swell" refers to waves that have progressed beyond the influence of the generating winds. Swell waves are comparatively long in period, their crests are rounded and usually lower than sea waves, and they are more uniform in height and direction. The direction of swell is independent of the local wind direction but is essentially the direction of the parent waves when they departed from the generating area. Generally, sea and swell are present in an area at the same time, though on occasion one may obscure the other.

The sea surface actually consists of a range of differing wave heights. However, by visual observation one usually is capable of estimating only a single wave height to describe sea, swell, or waves. The estimate of wave height is based on the average height of the highest one-third of all waves present at a given time and place; this is the concept of "significant" height.

It is believed that an observer's judgment is biased toward the higher waves, which tend to have about the same height as significant waves. Similarly, visual observation is capable of estimating only a predominant wave period and direction.

3. Sea Surface Energy Spectrum

In modern practice the sea surface is described by its energy spectrum, that is, the distribution of energy in the various frequency components making up the sea surface. Figure 21 shows theoretical spectra of wave heights, which are proportional to energy, and wave periods for fully arisen seas with wind speeds of 20, 30, and 40 knots. Wave spectra for various wind speeds, wind durations, and fetch distances have not been fully established. Research is still underway to define these spectra more precisely and to develop a better understanding of how the energy of waves is distributed in regard to the direction of propagation. Instrumental observations are required to provide the information from which wave spectra can be determined.

4. Correlation of Wind Speeds and Sea State

The Oceanographic Atlas[18] also presents state-of-the-sea charts for the various months of the year. Since waves are dependent primarily upon wind force it is of interest to see if there is a close relationship between the observed sea-state and wind-speed distributions. To facilitate comparison it is necessary to transform the sea-state distributions to equivalent wind-force distributions. Table VII shows the Wenz sea criteria of wind speed, wave height, and sea state and the Oceanographic Atlas

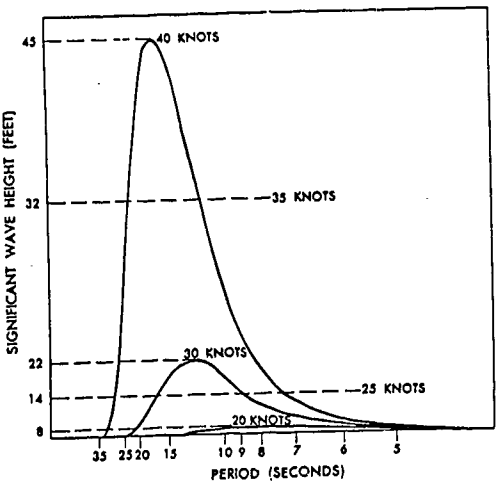

Fig. 21 Wave spectrum curves.[18]

Table VII

Approximate Relation Between Wenz[19] Sea Criteria of Wind Speed, Wave Height and Sea State, and the Oceanographic Atlas[18] Sea Criteria of Wave Height and "State-of-the-Sea"

Sea Criteria			Beaufort Scale	Wind Speed Range (knots)	Mean Knots	Sea State Scale	12-h Wind Wave Height (ft)*†	Fully Arisen Sea		
Atlas	Wave Height	Wenz						Wave Height (ft)*†	Duration h †‡	Fetch†‡ naut. miles
Calm	-	Mirror-like	0	<1	-	0	-	-	-	-
		Ripples	1	1-3	2	½	-	-	-	-
Slight	<3 ft	Small wavelets	2	4-6	5	1	<1	<1	-	-
		Large wavelets, scattered white caps	3	7-10	8½	2	1-2	1-2	<2.5	<10
Moderate	3-5 ft	Small waves, frequent white caps	4	11-16	13½	3	2-5	2-6	2.5-6.5	10-40
Rough	5-8 ft	Moderate waves, many white caps	5	17-21	19	4	5-8	6-10	6.5-11	40-100
Very rough	8-12 ft	Large waves, white caps everywhere, spray	6	22-27	24½	5	8-12	10-17	11-18	100-200
High	≥12 ft	Heaped-up sea, blown spray, streaks	7	28-33	30½	6	12-17	17-26	18-29	200-400
		Moderately high, long waves, spindrift	≥8	34-(>40)	37	≥7	17-(>24)	26-(>39)	29-(>42)	400-(>700)

* The average height of the highest one-third of the waves (significant wave height).

† Estimated by Wenz[19] from data given in U.S. Hydrographic Office Publications HO 604 (1951) and HO 603 (1955).

‡ The minimum fetch and duration of the wind needed to generate a fully arisen sea. Fetch refers to ocean path distance, in nautical miles, over which the wind is blowing.

sea criteria for wave height. A comparison of the Wenz wave height with the Atlas reveals some differences for the case of the "fully arisen sea." However, the Wenz and Atlas wave heights are approximately equivalent for the 12-hour wind criterion. It appears that the Atlas sea criteria on wave height deal only with waves generated by winds of 12-hour duration.

The Atlas sea criteria can then be transformed into the corresponding Wenz parameters of wind-force Beaufort numbers, wind-speed ranges, and wind durations of 12 hours. This transformation has been done in Table VIII, which shows the approximate Beaufort scale and approximate wind-speed range (in knots), approximate sea-state number, and corresponding wave heights and cumulative frequency data (Oceanographic Atlas) for all the months of the year. The yearly median (unweighted) is also shown for the wave-height range and corresponding wind-speed range. Weighting does not appear necessary here since the number of observations for each month are approximately equal.

Figure 22 shows the cumulative frequency distribtuion for the sea-state data (wave heights) transformed into equivalent wind-speed values of Table VIII, also shown is the wind-speed distribution curve derived previously from the wind-speed data of Table VI at the same geographical coordinates. Comparison of the two curves shows a good degree of correlation between the Atlas[18] data derived from observations of wind speeds and from observations of wave heights. However, it is not safe to draw the general conclusion that this will be so for all situations and locations. Wind speed alone is a crude and incomplete measurement of the surface agitation (see Table VIII). Surface agitation depends also on such

Table VIII

Cumulative Distribution Data For Approximate Corresponding Beaufort Wind Force Scale, Sea State Scale, and Wind Speed Range as Related to Oceanographic Atlas[18] Data on State-of-the-Sea Wave Height at 33° N, 67° W

State of the Sea Wave Height (ft)	Approx. Sea State Number	Approx. Beaufort Wind Force Number	Approx. Wind Speed Range (Knots)	Jan	Feb	Mar	Apr	May	Jun	Jul	Aug	Sep	Oct	Nov	Dec	Yearly Median (Unweighted)
calm	0-½	0-1	0-3	2%	1%	2%	2%	6%	6%	5%	7%	7%	3%	3%	2%	3.8
<3 ft (slight)	1-2	2-3	4-10	41	34	37	48	65	68	69	69	64	49	41	54	54.0
3-5 ft (moderate)	3	4	11-16	66	59	66	74	86	89	90	91	85	75	69	82	77.6
5-8 ft (rough)	4	5	17-21	31	78	83	90	96	98	98	98	96	91	84	92	90.5
8-12 ft (very rough)	5	6	22-27	92	91	94	95	99	99.99	99.99	99.99	98	97	96	99.99	96.8
≥12 ft (high)	≥6	≥7	≥28	99.99	99.99	96	99.99	99.99					99.99	99.99		
		Number of Samples		1616	1506	1760	1547	1448	1533	1663	1490	1656	1518	1486	1536	

UNCLASSIFIED

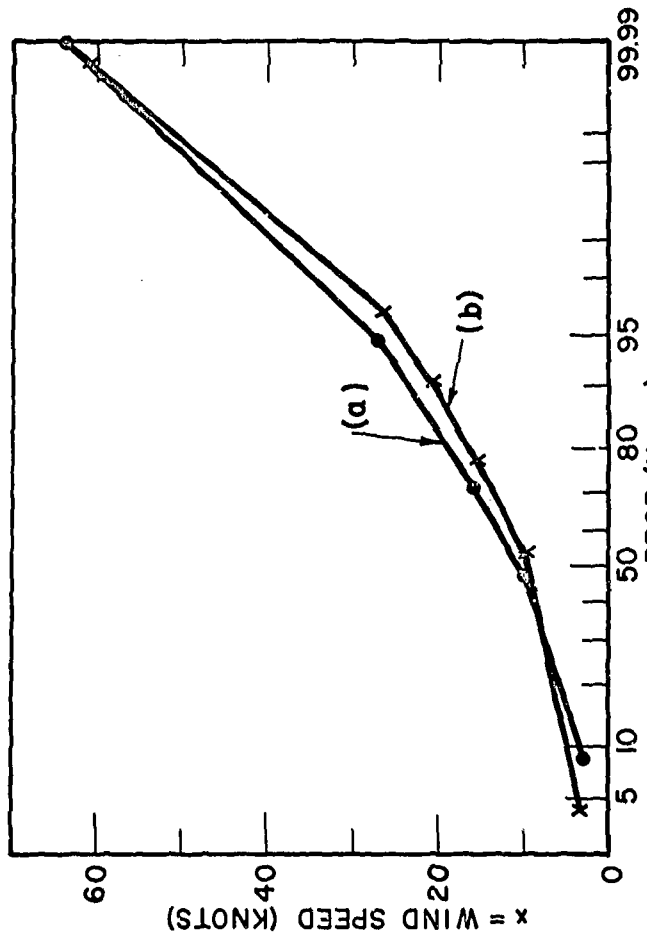

Fig. 22 Wind speed distribution (weighted) for wind rose at 33° N, 67° W. For curve (a) mean = 11 knots, std. deviation = 10 knots. For curve (b) mean = 10 knots, std. deviation = 8 knots.

factors as the duration, fetch, and constancy of the wind, and its direction in relation to local conditions of swell, current, and, in near-shore areas, topography. Subjective estimates of sea state by an observer are not necessarily an improvement over wind speed as a measure of surface agitation. For more on "wave forcasting" and discussion of "significant height method" and the "wave spectra method," refer to the tutorial paper by C. L. Bretschneider.[33]

5. Correlation of Ambient Noise Levels with Wind Speed and Wave Height

Figure 23 shows the correlation of ambient noise level with wind speed, and also wind speed with wave height. Each point is based on approximately 4500 observations,[22] over a 24-hour period. It is indicated here that wind speed is more closely correlated to the ambient noise level than is the wave height down to about 200 Hz. The effects of the wind on the sea surface are most pronounced at frequencies greater than 300 to 400 Hz.

Table IX generalizes the results of observations by V. Cornish[34] on the maximum dimensions of recurrent waves formed by winds of different speeds upon the open ocean far from the windward shore. The speeds are given in statute miles per hour; these must be converted to nautical miles per hour. An empirical formula by T. Stevenson for relation of maximum wave height to length of fetch, "Height = 1.5 × square root of length of fetch in nautical miles," provides estimates which approximate the wave-height observations of Table IX and the wave heights shown in Table VII for a fully arisen sea. It should be noted that although the data of Table IX are over 35 years old they provide some rough approximations (still used today)

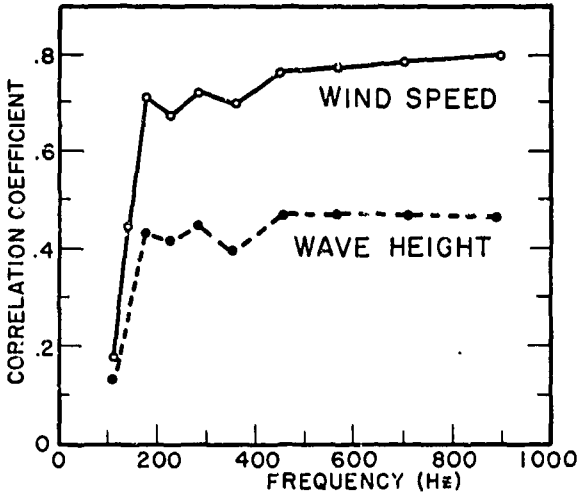

Fig. 23 Correlation of ambient noise level with wind speed, wave height.[22]

Table IX

Maximum Dimensions of the Recurrent Waves

of the Ocean in Relation to Speed of Wind[34]

Beaufort number	Speed of wind statute miles per hour	Speed of wave statute miles per hour = 8/10 speed of wind	Period (secs) = speed of wave ÷ $3\frac{1}{2}$	Length (ft) = square of period × 5 1/8	Height (ft) = 7/10 speed of wind	Length/ Height = period × 1 2/3
$6\frac{1}{2}$	31	24.8	7.0	251	21.7	11.6
7	35	28.0	8.0	328	24.5	13.3
8	42	33.6	9.6	472	29.4	16.0
9	50	40.0	11.4	666	35.0	19.0
10	59	47.2	13.5	934	41.3	22.6
11	68	54.4	15.5	1231	47.6	25.9

of the relationship between wind speed, speed of wave, wave period, and wavelength and height. For a more comprehensive treatment we go to the referenced paper by C. L. Bretschneider.[33]

6. Estimating Wind-Generated Noise

Figure 24 shows Artemis noise spectrum levels by Arase et al. for frequencies of 225, 450, 900, and 1400 Hz as measured with an omni-directional hydrophone. The scatter of the mean levels about the smooth lines are relatively small; this indicates a good correlation between the wind speed and ambient noise levels. The standard deviations of the mean noise level are small at the high noise levels and larger at the low noise levels. This is attributed, by Arase et al., to the presence of system noise (only in the 900 and 1400 Hz bands) and to the possible presence of undetected noise sources.

Figure 25 shows a set of curves (by Arase[35]) of ambient noise spectrum levels versus wind speed and sea state as observed during 1963-1965; the corresponding values of Beaufort wind force have also been added. The curves shown are in reasonably good agreement with those of Figure 24 and Figure 4 and Wenz's[19] wind speed - noise curves: Figure 26 and A. D. Little's[10] curves.* (See Table X for another comparison of wind speeds and noise levels.)

Referring back to Figure 19 note that the mean estimate of wind speed derived from the Atlas[18] data is 11 knots; this falls within the Beaufort wind-force number 4 which is the same wind-force number estimated for the measured Artemis data. Using the wind-force Beaufort No. 4 the ambient noise level is estimated as -36 dB/1μbar for a frequency

* See Figure 27.

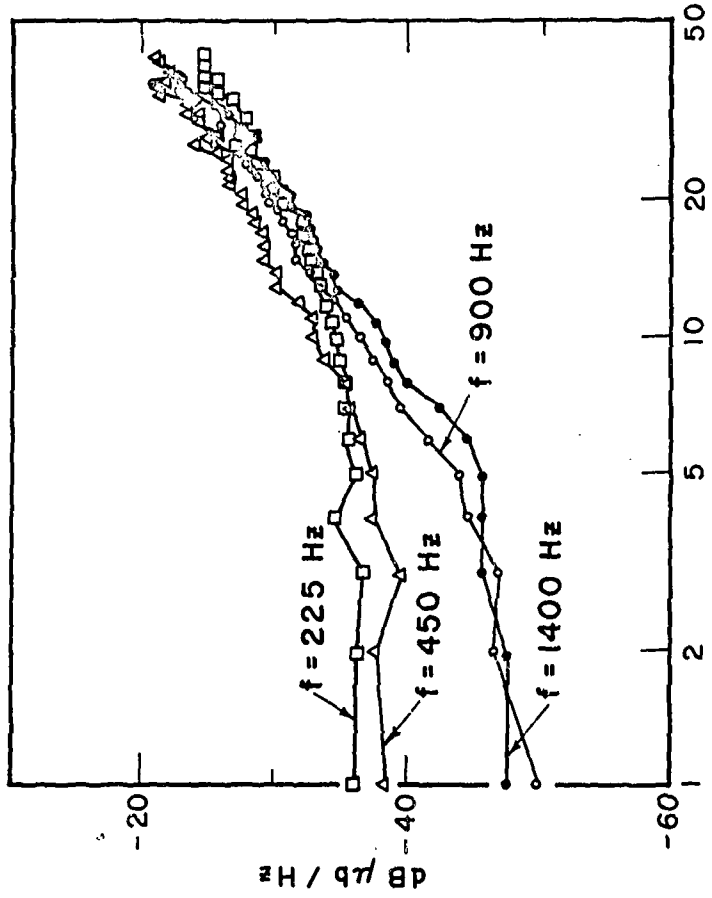

Fig. 24 Ambient noise spectrum levels at 225, 450, 900, and 1400 Hz.[8]

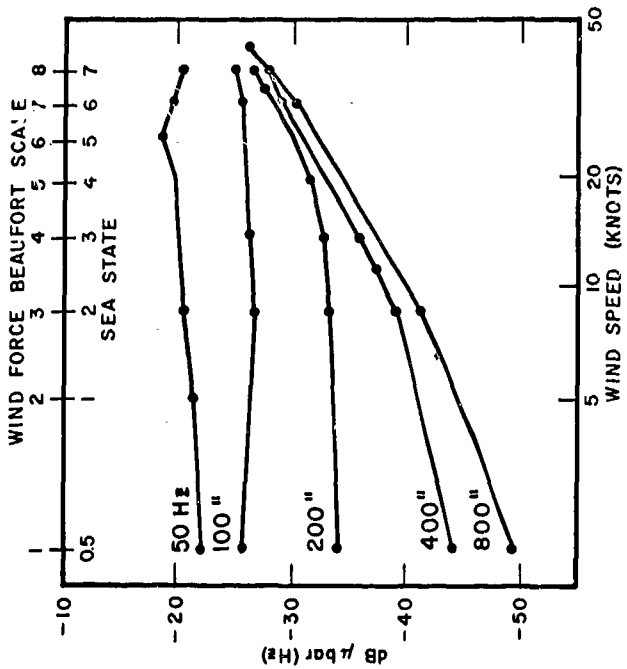

Fig. 25 Ambient noise spectrum levels vs. wind speed, sea state, and wind force Beaufort numbers.

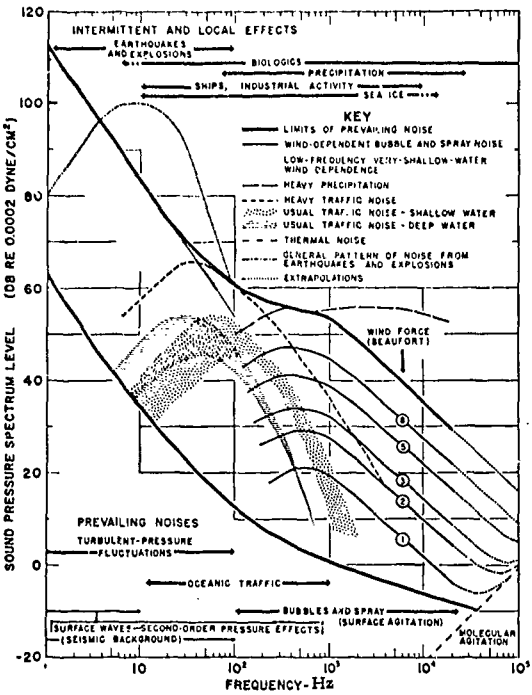

Fig. 26 Composite of ambient noise spectra (from Wenz[19]).

Table X

Some Comparisons of Wind Speeds

and Respective Noise Levels

	Reference 22		Reference 28	
Month	Wind Speed Knots	Noise at 446 Hz dB//1 µbar	Wind Speed Knots	Noise at 400 Hz dB//1 µbar
Jan	18.5	-28	15.-	-36
Feb	19	-26.5	17.4	-32.6
Mar	18.5	-30.5	-	-
April	16.5	-30.5	15.-	-30.5
May	13	-34.5	17.5	-34.7
June	12.5	-35	-	-
July	12.5	-36	-	-
Aug	10	-37	7.5	-39.5
Sep	10.5	-32.5	-	-
Oct	16	-30	-	-
Nov	18.2	-30.5	-	-
Dec	.8	-28	17.4	-37.8
Total	170.7	379	89.8	210.78
Average	14.2	-31.6	14.97	-35.13

of 400 Hz. If we use the peak value as the wind speed of 11 knots, we find the ambient noise level to be -37 dB/1 μbar. This is about 3 to 4 dB lower than the value shown by Weigle and Perrone[6] (see Fig. 7). It may be concluded that wind-generated noise estimates for the Artemis area are within 3 to 4 dB of measured noise levels. This is reasonably close enough for estimating wind-generated noise levels. (C)

PREDICTION OF OCEANIC TRAFFIC NOISE

The magnitude of oceanic traffic noise that may be expected at a particular hydrophone receiver array will be determined by the average transmission loss over the underwater path, the number of ships, and the distribution of these ships. Although the noise source characteristics depend on the nature of the ship source, the base is so broad for a larger number of ships (ten or more) that the individual source differences blend into an average source characteristic. This oceanic traffic noise is a significant element of the observed ambient noise at frequencies below 178 Hz; below this frequency the observed ambient noise is not strongly wind dependent. At higher frequencies such as 200-500 Hz the oceanic traffic noise may also be significant at low wind speeds, say below 5 knots.

For most surface ships, the effective source of the radiated noise is between 10 and 30 ft below the ocean surface. Up to frequencies of 50 Hz, the source and its image from surface reflection operate as an acoustic doublet; noise is radiated with a spectrum slope of +6 dB per octave relative to the spectrum of the simple source.

Wenz[19] obtains some notion of the probable shape of traffic noise spectra by deriving the curves shown in Fig. 27. The variations in the spectra caused by differences in source depth and differences in the attenuation at different ranges are indicated by the composite set of curves. The effect of source depth at low frequencies is shown by the curves numbered (1) for a depth of 20 ft, and (2) for 10 ft. The choices of source-noise spectrum shape, based on the data recorded by Dow,[36] are described in terms of the slopes of the sound-pressure-level spectra. The resulting curves are

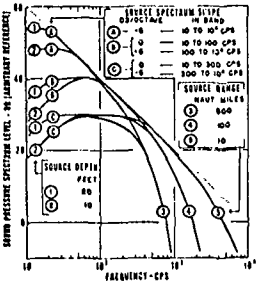

Fig. 27 Traffic-noise spectra deduced by Wenz[19] from ship-noise source characteristics and attenuation effects.

defined as follows: (A) -6 dB per octave, (B) 0 dB per octave up to 100 Hz, and (C) 0 dB per octave up to 300 Hz and -6 dB per octave above 300 Hz. The change in the spectrum shape as the range varies, due to attenuation, is shown by curve (3) representing a range of 500 miles, curve (4) a range of 100 miles, and curve (5) a range of 10 miles. The spectrum corresponding to a particular set of conditions may be found by following the curves identified by the relevant numbers and letter. For example, the curve 1 B4 is the spectrum form which would be observed at 100 miles from a source located at a depth of 20 ft, and whose spectrum is flat up to 100 Hz and decreases at 6 dB per octave above 100 Hz.

Note that the source spectrum shape is altered in transmission by the frequency-dependent attenuation* part of the transmission loss. Wenz[19] in his derivation of the curves of Fig. 27 uses Sheely and Halley's attenuation factor of $0.066\ f^{3/2}$ dB per nautical mile, where f is the frequency in Hz. At long ranges the attenuation increases rapidly with frequency above 500 Hz.

It has been shown by Hale[38] that experimental results from long-range transmission in deep water do not fit the free field, spherical divergence law very well; better agreement with experiment is shown to result if the boundaries and sound velocity structure are taken into account.

Table XI is from Weigle's and Perrone's report[6] on ambient noise in the Artemis area; the table shows the results of two studies[39,40] of ship traffic density that are pertinent to the Artemis area. (C)

---

* This does not include spreading loss, which is independent of frequency.

Table XI

Comparison of the Studies on Ship Traffic Density[6]

Range (nautical miles)	No. of Ships Per Degree		No. of Ships Per 60 Degree Sector	
	Reference 39	Reference 40	Reference 39	Reference 40
0-150	.017	.055	1.20	3.31
150-250	.017	.120	1.02	7.25
250-350	.130	.224	7.80	13.44
350-450	.300	.320	18.00	19.21
450-550	.350	.460	21.00	27.61
550-650	.500	.541	30.00	32.47

From the data of Table XI when they are equally weighted, there is obtained an expectation of 1.51 ships/degree in the Artemis sector and a mean ship range of 475 miles. (C)

In the 60-degree sector of major interest there are then a total of 103 ships at a mean range* of 475 miles. Each of these ships is considered as a noice source[36] with an output level at 1 yd of approximately 63 dB//1 μbar/Hz ± 10 dB at 100 Hz and with a spectrum slope of -6 dB/ octave. A power addition of the outputs of 100 ships results in effective source levels of approximately 83 dB//1 μbar/Hz at 100 Hz and 77 dB//1 μbar/ Hz at 200 Hz. (C)

Long-range acoustic loss measurements at 400 Hz of the Artemis receivers indicate a total expected loss of approximately 122 dB from a range of 475 miles. The attenuation portion of the total loss for 400 Hz amounts to 13.7 dB[41] which leaves 108 dB for propagation losses exclusive of attenuation. According to Thorp,[41] the expected attenuation values over the 475-mile range for 100 and 200 Hz are 1.7 and 4.8 respectively. Therefore, the expected received traffic noise level at the Artemis receiver field is approximately -26.7 dB//1 μbar/Hz at 100 Hz and -35.8 dB//1 μbar/Hz at 200 Hz, and -51 dB// 1 μbar/Hz at 400 Hz. (C)

(C) Figure 28 compares these values up to 200 Hz with the mean noise levels measured at the Artemis receivers under the lowest wind speed condition (0-5 knots). It is noted that Fig. 28 shows level differences up to 4.5 dB and some slope differences. However, Weigle and Perrone[6] contend that the agreement is well within the uncertainity of the ship's source

* In general, we cannot take average range as typical, since propagation loss (in dB) is not linear with range; e.g., for 500 miles at 400 Hz the convergent zone transmission loss is 117 dB.

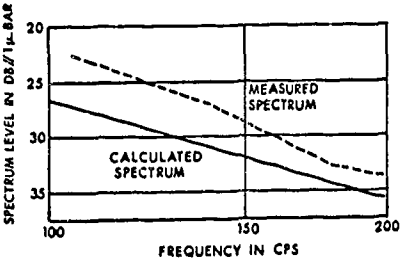

Fig. 28 Distant traffic noise spectra.[6]

level estimates and that this tends to support the thesis that ambient noise observed at low wind speeds in this frequency range has its origin in distant ocean traffic. (C)

Figure 29 presents A. D. Little Co.'s[28] idealized average ambient noise spectra based on the dominance of shipping noise below 200 to 300 Hz and of sea noise above this frequency region. Using the curves of Fig. 29 one may roughly approximate* the ambient noise, at any location and at any season, by selecting the appropriate shipping and sea noise curves and blending them together in the middle frequencies. (C)

Table XII indicates the shipping noise curves corresponding to some ocean areas and seasons of the year. The list is limited in the number of areas indicated; also the seasons are not indicated for some of the areas probably because of lack of data for all seasons.

Note from Table XII and Fig. 29 that the shipping noise curve, for the remote parts of the Atlantic, varies from as low as "C" in the summer, to as high as "E" in the winter; the "D" curve may be considered to be close to the average for the year. Around Bermuda, the levels run about a half letter higher. In the coastal areas (where shipping lanes are important) the average level is between "E" and "F." Curve G is the highest level of shipping noise that could occur; however, this may be representative of "near ship noise" in which the individual ships are close to the receiver arrays. (C)

In very quiet areas, remote from shipping, the levels are as low as curve "B" or curve "A."

---

* The uncertainty of ship noise level is about 10 dB.

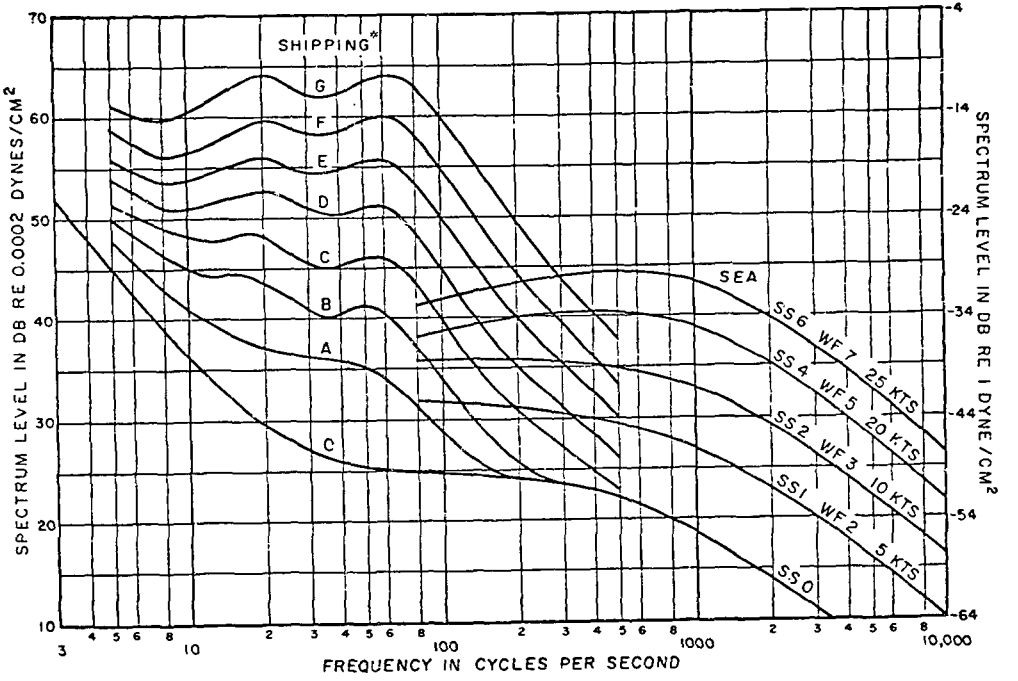

Fig. 29 Idealized average spectrum of ambient noise (1962) from Ref. 28.

*See following Table XII for correspondence of shipping curves with ocean areas.

Table XII

Underwater Ship Traffic Noise Types in Certain Areas[28]

Area	Season	Curve Type
Eleuthera	Average	D
Eleuthera	Summer	C to D
Eleuthera	Winter	E
Bermuda	Average	D to E
Bermuda	Summer	D
Bermuda	Winter	E to F
Very deep SE Bermuda	Fall	C
Very deep W Bermuda	Fall	F
Puerto Rico	Winter	D
Grand Turk Island	Summer	C to D
San Salvador	Spring	C
Lesser Antilles	Summer	C
Lesser Antilles	Fall	C
Capes May and Hatteras	-	E to F
Nantucket Area	-	E to F
North of Seattle	-	C to D
Cape Mendocino	-	D
Capo Blanco	-	E to F
Tongue-of-the-Ocean	-	B
New Zealand	-	A
Bearing Straits	-	B to C

The curves in Fig. 29 are useful in roughly estimating average oceanic traffic noise, sea noise, and the composite noise levels. However, such estimates are only a rough approximation. For more accurate estimates of averages it is necessary to incorporate any available experimental data, and ship traffic data for a particular area of interest.

PREDICTION OF BIOLOGICAL NOISE LEVELS

It is difficult if not impossible to predict an average level of biological noise for any area. Noise from marine animals is very variable in spectral and temporal characteristics; the statistics of such noise involve a nonstationary process. The magnitude and other characteristics of such noise will vary by area, year, season, and time of day. Also, while many types of marine organisms are known to produce sound, it has not been possible to relate all the sounds heard to the particular marine animals that make them.

1. Marine Animal Noise in Coastal Areas

In coastal waters two types of marine animals, snapping shrimp and croakers, appear to be the most likely sources of biological noise. Shrimp are common in shallow, hard-bottomed tropical water, whereas croakers occur in such areas as Chesapeake and other east coast bays; croakers occur to a lesser extent on the Pacific coast. Figure 30 shows some typical ambient-noise levels produced by croakers and snapping shrimp;[42] these levels will vary according to time of day and season of the year. In general one might assume that marine biological noise produced in coastal areas is not of concern to deep water surveillance systems. However, some deep water hydrophone receiver arrays may be located near a coastal area where propagation conditions might favor the reception of shrimp and coastal noise. This means that location of receiver arrays for deep water surveillance systems should not discount entirely the effects of marine animal noise from relatively close (i.e., propagation-wise) coastal areas.

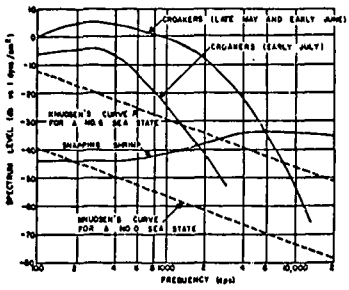

Fig. 30 Ambient-noise levels produced by croakers and snapping shrimp.[42]

Other sources of marine animal noise in coastal waters have been attributed to mussels, barnacles, sea urchins, toadfishes, and catfishes. Cetaceans (whales and porpoises) sometimes occur in coastal areas; however, since cetacean noise is more prevalent in some deep water areas it will be discussed separately in the next paragraph. For a summary of the characteristics of various marine animal noise sources in coastal areas see Table XIII.

2. Marine Animal Noise in the Deep Ocean

In the deep ocean the chief noisemakers are the cetaceans, (i.e., whales and porpoises). In general, the cetacean noise signals produce temporary changes in noise levels; that is the sound making is not a continuous noise. However, in many instances the cetacean signals are of sufficient amplitude and duration to raise the ambient noise level past tolerable limits.

In the Artemis area it was found[22] that noise limiting occurred about 70% of the time during a 12-hour period of intense activity. This may be expected on breeding or feeding grounds where cetaceans may tarry and congregate; in such instances, it may be said that sound making may be continuous over a continuous period of time. Noise from whales appears to be a seasonal problem with the worst conditions, in the Artemis area, persisting over the last three or four weeks in April. Greatest whale noise occurs from dusk to dawn during the period of whale activity. Whale noise of large magnitude has been found to occur in the 224, 446, 891, and 1414 Hz frequency bands (refer back to Fig. 3), the noisest of the four frequency bands being 224 Hz. Whale-noise to sea-noise ratios ranged to a maximum of 27 dB; ratios of 8 dB were the most frequent. (C)

Table XIII

Some Biological Sources of Sustained Ambient Sea Noise

Marine Animal Source	Type of Coastal Area	Geographical Occurrence (or where heard)	Depth	Frequency Range	Source Sound Pressure Level (dB//1 μbar)	Diurnal Variation	Seasonal Variation
Snapping Shrimps	Tropical shallow water	In global belt bounded by 40°N and 40°S latitudes	(≤ 30 fath.)	100 Hz - 20 kHz	55 dB	Max. at night Peaks after sunset	Little seasonal variation
Croakers	Pacific and Atlantic coastal waters	Harbors, bays	Not given	350-1500 Hz	40 dB peak	Starts at 0700 Max. at 2200 Finish at 0230	At Cape Henry, Va.; rose rapidly after mid-May and peaked during 3 weeks of June
Toadfishes	Shallow coastal waters	Maine to Cuba	Not given	250, 350 Hz	Not given	Not given	Begins late May and ends in early June
Catfishes	Harbors; not given for other coastal areas	Florida, South Carolina, Tokyo Harbor		75-150 Hz, 800-1600 Hz, 300-600 Hz	Max. in 300-600 Hz band; dB not given	Not given	Not given
Sea Urchins	Pacific and Atlantic coastal waters	New Zealand, Bimini, etc.	Not given	30-5000 Hz	-60 dE in 1/3-octave band at 1600 Hz; group "chorus" at -25 dB	Begins (at 5 dB below max.) at about 22 min after sunset	Not given
Mussels	Atlantic tropical and temperate coastal waters	Narragansett Bay, Arctic to Cape Hatteras	≤ 60 ft	500 Hz - 4 kHz	90 dB	Max. at midday Min. after sunset	Max. during summer
Barnacles	Atlantic coast	Gloucester Point, Va., Narragansett, Mediterranian, etc.	Not given	500 Hz - 4 kHz	70 dB	Not known	Max. in September

Publications giving estimates of whale (and shark distributions) are listed as references 23-26 and 43. From such reference sources one may estimate the areas, expected magnitudes, and frequency of occurrence of whale-noise sources.

The magnitudes of whale noise should not be added in with the ambient noise level due to sea state and oceanic traffic to provide an average median yearly level.* However, the limiting effects of whale noise should be noted for certain times of the year and for certain ocean areas; this may be important in the selection of underwater receiver array sites.

* The whale noises are not continuous in nature and they are very seasonal in occurrence.

ESTIMATING THE COMPOSITE BACKGROUND OF AMBIENT NOISE

To determine the magnitudes of the ambient noise background levels in a particular ocean area it is necessary to estimate and combine the noise levels of the various contributory noise sources. In some instances one may only be interested in estimating the yearly median noise levels; however, in the evaluation of surveillance systems we also need to estimate the seasonal and monthly median levels; we may even need to consider, in the final analysis, diurnal noise level variations and such short term variations as hourly and sporadic variations. The difference between the yearly and monthly medians may be as much as 30 dB. There may also be certain days during the year, or hours during the day, where a surveillance "blackout" may occur due to a sudden onset of high noise levels; for such cases it is important to indicate the percentage of time in which a "blackout" could occur.

Suppose we are required to compare the effectiveness of some surveillance receiver arrays that are to be emplaced in a particular ocean area. The first step is to estimate the ambient noise background levels.

Assuming that the ambient noise background is the significant factor, we need to specify as much of the noise characteristics as possible. As an illustration a set of typical data sheets (Table XIV) has been prepared as an example. The particular ocean area in this case is he Artemis area off Bermuda; here we draw on the results of experimental measurements over a period of several years. However, in other ocean areas where few (or no) measurements have been made, we have no choice but

Ocean Area: Bermuda (Artemis Array)
Geographic Coordinates: 32° N, 63° W
Specific Frequency: 400 Hz

Table XIV

Ambient Noise Data Sheet

Type of Noise Source	Freq. Range	Yearly Median dB// 1 μbar	Seasonal Medians (dB)				Monthly Medians (dB)												Diurnal Variations	% Blackout (Noise Saturation)	Remarks
			Spring	Summer	Fall	Winter	Jan	Feb	Mar	Apr	May	Jun	Jul	Aug	Sep	Oct	Nov	Dec			
1) Oceanic Traffic Noise	10 Hz-1 kHz	-45 dB	-[a]	-46	-	-40	-	-	-	-	-	-	-	-	-	-	-	-	-	-	[a] No data available on monthly medians, diurnal etc.
2) Wind Generated Noise	100 Hz-20 kHz	-35 dB*	-35	37	-36	-34*	-34*	-33*	-34*	-35*	-36*	-36*	-36*	-38*	-38*	-35*	-34*	-34*	-[b]	-	* Indirect estimates of monthly median [b] Not applicable.
3) Precipitation	100 Hz-500 Hz	-[c]	-	-	-	-	-	-	-	-	-	-	-	-	-	-	-	-	no	no	[c] Add about 2 dB to noise level when precipitation occurs. However, high sea states usually mask rain effects.
4) Seismic	1 Hz-100 Hz	-[d]	-	-	-	-	-	-	-	-	-	-	-	-	-	-	-	-	-	-	[d] Transient, sporadic nature of seismic noise defies statistical prediction.
5) Thermal	>20 kHz	-[e]	-[e]	-	-	-	-	-	-	-	-	-	-	-	-	-	-	-	-	-	[e] Not significant at 400 Hz.
6) Sea - Ice	10 Hz-100 kHz	-[f]	-	-	-	-	-	-	-	-	-	-	-	-	-	-	-	-	-	-	[f] No ice in Bermuda area.
7) Biological	10 Hz-100 kHz	-[g]	-[h]	-	-	-	-	-	-	-	-	-	-	-	-	-	-	-	-	-	[g] No yearly median.
a) Shrimp		†																			
b) Toadfish		†																			
c) Whale		-	-[i]				-	-	-	i	-	-	-	-	-	-	-	-	Greatest during daytime	77% of time during one 12 hour period	[i] Greatest whale activity during month of April
d) Porpoise		†																			† No data on effects of other marine biological sources.
e) Other		†																			
	Total (Composite)			-37		-34															for 440 Hz.

to rely on indirect methods of estimating noise levels. For example we could use the Oceanographic Atlas charts[18] to estimate the wind forces and then deduce the noise levels; or we could use ship traffic data to estimate the average oceanic traffic noise. When using indirect means of estimating noise levels, we identify them by an asterisk (*).

DIRECTIONAL PROPERTIES AND SPACE TIME OF AMBIENT NOISE

Space-Time Correlations

Some recent papers of interest on the subject of space-time correlations of ambient noise are by R. J. Urick,[34] E. M. Arase, T. Arase,[5,14] W. Liggett, M. Jacobson,[46] and D. Lytle, P. Moose.[47]

Urick hypothesizes an admixture of two different noise types in a "mix" that depends on sea state and frequency. In the Urick study time-delay correlograms were obtained in two frequency bands (200-400 Hz and 1-2 kHz), over a range of wind speeds and hydrophone separation; a 40-element vertical array was used at Bermuda. The hydrophones were at a depth of 14,500 ft.

Figure 31 shows ambient-noise correlograms in the octave 200-400 Hz for a number of different separations and wind speeds. The autocorrelogram from a single hydrophone, with paralleled inputs to the correlator, is shown at the bottom of the figure; in the sequence above, it corresponds to a separation of 0 ft. Figure 32 is a similar set of correlograms for the octave 1-2 kHz.

The correlograms fall into two broad classes. Referring to Fig. 31 (200-400Hz), the correlograms at a wind speed of 4 knots show a high peak value that remains nearly centered at 0 delay, even for the highest separation of 23.1 ft; these are called Type I. At wind speeds of 25-30 knots, the correlogram peak diminishes in amplitude and moves outward in time delay as the separation increases. These correlograms are called Type II. At intermediate wind speeds, the correlograms suggest mixtures

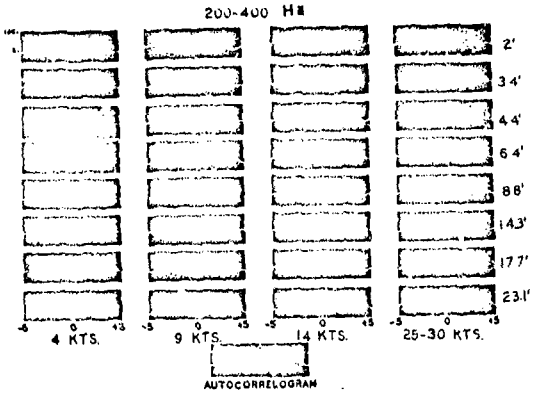

Fig. 31 Time delay correlograms in the octave 200-400Hz for various wind speeds and vertical hydrophone separations.[34]

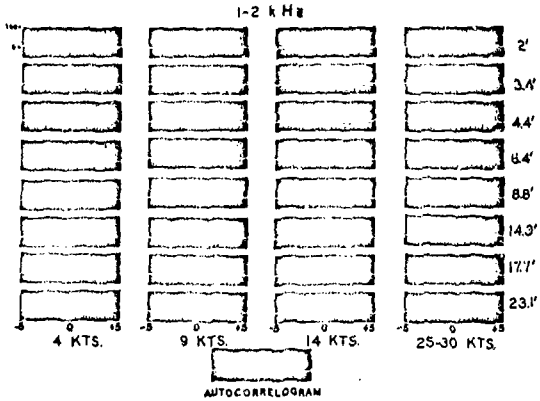

Fig. 32 Time delay correlograms in the octave 1-2 kHz for various wind speeds and vertical hydrophone separations.[34]

of the two basic types. In Fig. 32 (1-2 kHz), the correlograms are all Type II, except possibly at the 4-knot wind speed. Figure 33 shows the distribution of the two correlogram types on a plot having wind speed and frequency as coordinates.

In terms of the ambient noise that generates them, Urick interprets the correlograms as indicating two different kinds of noise. The noise generating the Type I correlograms is interpreted as arriving horizontally at the array; it maintains a high coherence at 0 time delay over relatively large separations in the vertical. One source of this noise is ship traffic many miles away. This noise is dominant at low frequencies and low wind speeds (Fig. 33). Type II noise* is postulated to originate at the sea surface, and to become the dominant source of noise at high frequencies and high wind speeds. Figure 34 is a diagrammatic visualization of these two kinds of noise.

The evidence that the Type II noise originates at the sea surface is sought in a comparison of the theoretical correlation of sea-surface noise with the observed correlograms. The correlative properties of sea-surface noise have been investigated by Edie,[44] Liggett and Jacobson[45,46] and by Lytle and Moose.[47] Figure 35 shows a comparison between contour maps of correlation coefficient plotted against normalized time delay $\tau/(d/c)$, where τ is the time delay, d the distance between two vertically separated receivers, and c the velocity of sound; and against normalized separation d/T_g, where T_g is the geometric mean wavelength of the frequency band considered. The contour map on the left is computed

* This type of noise (Type II) has a much lower correlation coefficient because the noise source is distributed over an area that is orthogonal to the vertical axis of the hydrophone module.

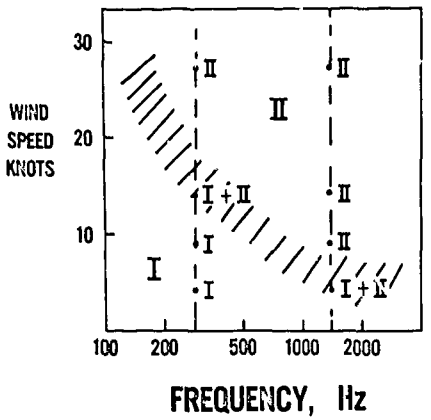

Fig. 33 Correlogram types as dependent on wind speed and frequency.[34]

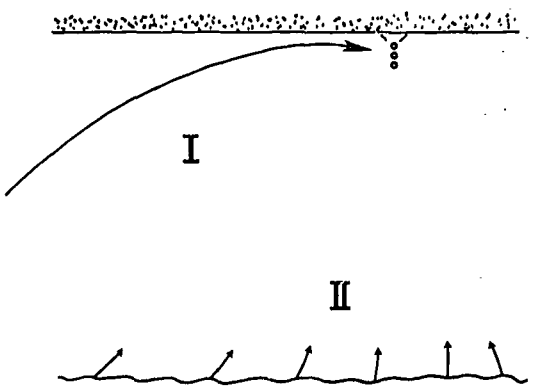

Fig. 34 Simple visualization of two kinds of ambient noise.[34]

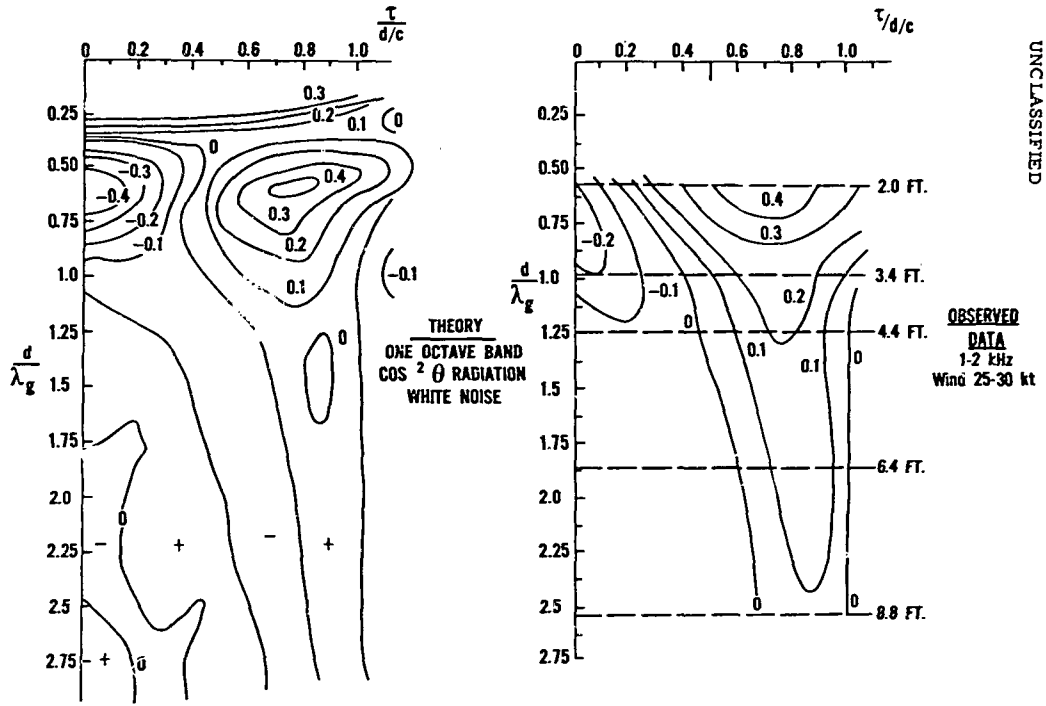

Fig. 35 Theoretical and observed contour maps of ambient-noise correlation coefficient on normalized coordinates of time delay (horizontally) and separation (vertically).[34]

theoretically by Edie for a 1-octave band of white noise, with $\cos^2\theta$ intensity-radiation pattern, from each elemental radiating area of sea surface, corresponding to a surface distribution of dipoles. The right-hand contour map is drawn from the values of the clipped correlation coefficient read from the 1- to 2-kHz correlograms of Fig. 32 for a wind speed of 25-30 knots. The similarity of the two patterns indicates that the interpretation of Type II noise as having a sea-surface origin may be valid.

Urick shows how such correlograms may be used in array design to discriminate against ambient noise by working out the following example.

(1) Example: To compute the improvements in S/N ratio to be expected from a 4-element, linear additive vertical array of equally spaced elements 5 ft apart, the ambient noise environment is said to be identical to that at Bermuda. It is assumed that the signal is perfectly coherent, with unit correlation coefficient between all elements of the array for all steering directions.

The array gain (AG), in decibel notation, is defined by:

$$AG = 10 \log [(S/N)_o/(S/N)_1] \qquad (1)$$

where $(S/N)_o$ denotes the ratio of signal power to noise power at the output of the array, and where $(S/N)_1$ is the same ratio at the output of a single element. Then for a linear additive array of n identical elements, the array gain is shown to be

$$AG = 10 \log \left[\sum_{j=1}^{n} \sum_{i=1}^{n} (\rho_s)_{ij} \Big/ \sum_{j=1}^{n} \sum_{i=1}^{n} (\rho_n)_{ij} \right] \qquad (2)$$

where $(\rho_s)_{ij}$ is the cross-correlation coefficient, or normalized time-averaged product, of the signal between the ith and the jth element of the array, and $(\rho_n)_{ij}$ is the cross-correlation coefficient of the noise. In taking the ρ's, the time delays needed to steer the array in the direction of the signal - and so maximize the numerator - must be included. By the assumption of perfect signal coherence in the example chosen, $(\rho_s)_{ij} = 1$ for all i,j the numerator in the above expression reduced to n^2. In the denominator, the various (ρ_n)'s are determined by the spatial coherence of the noise background.

Figure 36 shows the clipped correlation coefficient of the ambient noise at Bermuda plotted against separation distance d in feet, as read from the correlograms for the 200- to 400-Hz band. Carrying through the double summation in the denominator of the array gain expression, using values of ρ from the same figure for values of d equal to 5, 10, and 15 ft, one finds for horizontal steering an array gain of 1.5 dB at a 4-knot wind speed and 6.2 dB at a 25- to 30-knot wind speed; for a steering angle of 60° to the horizontal, the array gain is computed to be 5.6 dB at 4 knots and 2.9 dB at 25-30 knots.

Urick states that if unclipped, rather than clipped, correlation coefficients were used in the computation, only slightly different values of array gain would be found.* With horizontal steering at the low wind speed, the array gain is low because of the high noise correlation at time delays near 0 corresponding to the horizontal steering direction. At the

* However, C. N. Pryor[48] in a recent paper also shows that an error in apparent signal-arrival time may occur when a clipped array is used in nonuniform noise field; and that this error may become large enough under some conditions to limit the usefulness of clipped array processing in a nonuniform noise field.

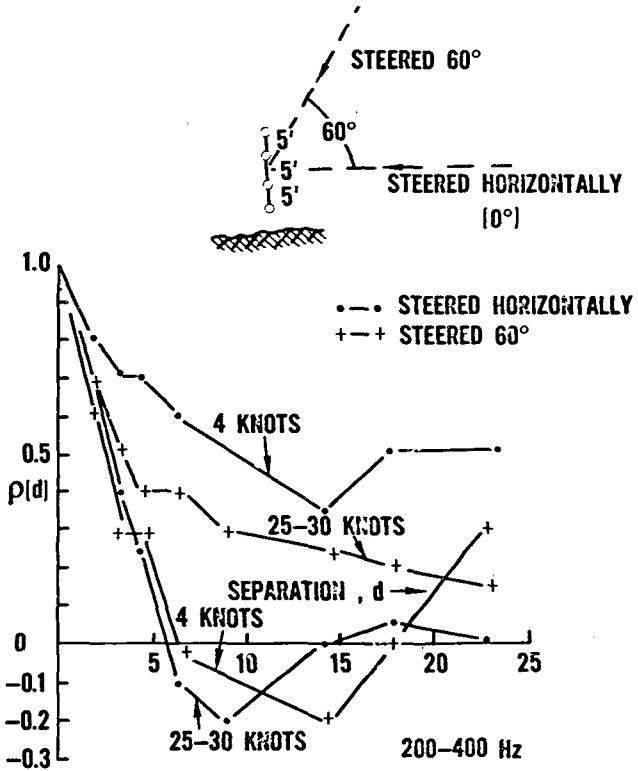

Fig. 36 Clipped correlation coefficient as read from correlgrams plotted against separation in feet for two wind speeds and two steering arrays. The upper figure illustrates the simple array considered in an example.[34]

60° steering angle at the high wind speed, the array gain is also low because of the coherence of noise at time delays corresponding to this angle. The above values may be compared with the array gain of $10 \log 4 = 6$ dB that would be found with uncorrelated noise. This example illustrates the precept that the gain of a linear additive array depends upon the correlative characteristics of the signal (here assumed perfectly coherent) and of the noise environment in which the array must operate.

The ambient noise correlations for the same 40-element vertical array at Bermuda is interpreted by the Arases[14] in terms of sea surface noise radiated with an intensity proportional to $\cos^n \theta$; where $n = 0, \frac{1}{2}, 1, 2$ for different ranges of sea state and frequency. The Arases used a simple model proposed by Cron and Sherman[49,50] which is similar in concept to Talham's[51] description of measured noise directivity. Figure 37 illustrates the concept of surface and volume noise models; Fig. 38 shows the geometry for the volume noise model; Figs. 39 and 40 show the geometry for the surface-noise model with one receiver and two receivers, respectively.

In the surface-noise model a uniform distribution of noise sources is assumed on the surface of the ocean with an intensity radiation pattern:

$$g^2(\alpha) = \cos^{2n} \alpha$$

where α is the angle from the vertical. An equation for the cross-correlation coefficient was derived by Cron and Sherman.[49,50] The distance d between receivers was assumed to be small compared to the distance from the receiver to the ocean surface. The effect of bottom reflections on the correlation function was neglected for distances larger than 5 wavelengths

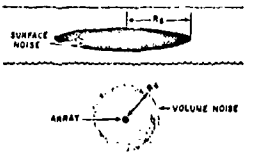

Fig. 37 Volume and surface noise models.[49]

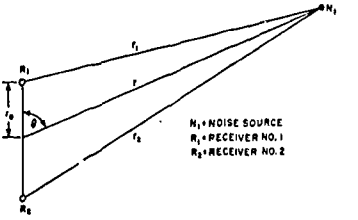

Fig. 38 Geometry for volume-noise model.[49]

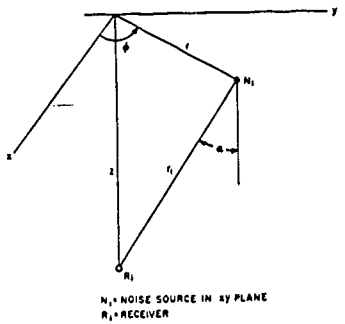

Fig. 39 Geometry for surface-noise model with one receiver.[49]

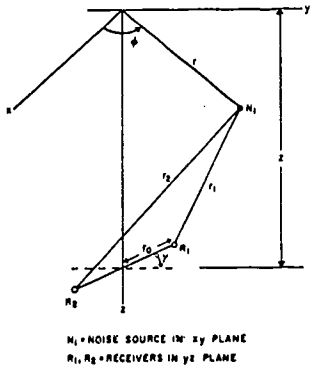

Fig. 40 Geometry for surface-noise model with two receivers.[49]

from the bottom; also, a constant sound velocity ocean was assumed. Radiation from the same noise source is assumed to correlate, while only the intensity adds for noise from different sources. For time delay τ, angle γ between the line joining the receivers and the surface, at a single circular frequency ω, the space-time correlation coefficient was found to be:

$$\rho(d, \tau, \gamma) = \frac{\int_0^{\pi/2} g^2(\alpha) \tan\alpha \cos(kd \sin\gamma \cos\alpha - \omega\tau)\, d\alpha}{\int_0^{\pi/2} g^2(\alpha) \tan\alpha\, d\alpha} \qquad (3)$$

Since noise is distributed in frequency and is filtered to obtain samples in frequency space, it is necessary to integrate over the frequency range. A summary of the equations used for horizontal and vertical receivers by the Arases[14] is given below for a flat spectrum between frequencies f_1 and f_2. This is in a slightly different form from that of Refs. 52 and 50 to make it more convenient for machine computation. The notation used was:

$$y = \frac{d}{\lambda} \quad ; \quad \psi = \frac{\tau c}{d} \quad ; \quad b^2 = \frac{f_2}{f_1}$$

where c is the velocity of sound and λ the wavelength. The case $\psi = 0$ corresponds to zero time delay.

For vertical receivers, with flat bandwidth Eq. 3 becomes:

$$\rho_n\left(y, \psi, \frac{\pi}{2}, b\right) = \frac{n}{\pi y\left(b - \frac{1}{b}\right)} \int_0^1 \frac{x^{2n-1}}{(x-\psi)} \left\{\sin\left[2\pi b y (x-\psi)\right] - \sin\left[\frac{2\pi y}{b}(x-\psi)\right]\right\} dx \qquad (4)$$

for $n \geq \frac{1}{2}$ and $y > 0$.

For horizontal receivers, with flat bandwidth Eq. 3 is therefore:

$$\rho_n (y, \psi, 0, b) = \frac{2^n n!}{2\pi y \left(b - \frac{1}{b}\right)} \int_{\frac{2\pi y}{b}}^{2\pi y b} \frac{J_n(x)}{x^n} \cos x \psi \, d x \qquad (5)$$

for $n = 0, \frac{1}{2}, 1 \ldots$ and $(m + \frac{1}{2})! = (\pi)^{1/2} \frac{1 \cdot 3 \ldots (2m+1)}{2^{m+1}}$

$$y > 0 \quad .$$

Note that the case for $n = 0$ corresponds to omnidirectional surface sources which violates a boundary condition that at a free surface the sound pressure is equal to zero. However, Talham[51] suggests another function which approximates the case for $n = 0$; the results are not said to be significantly different.

a. Correlations for Horizontal Elements

In the Artemis experiments by the Arases,[14] the spatial correlation was measured with horizontally separated hydrophones at 22, 32, 45, and 63 Hz for various sea states. The experimental values corrected for clipping are given in Figs. 41 through 44. Here the frequencies corresponding to the -3 dB points of the filter response had a ratio of 1.7 (except for the 400-Hz filter, where this ratio was 1.3); the actual response was therefore approximated by white noise within this frequency range and the theoretical curves were computed using Eq. (5) for $n = 0, \frac{1}{2}, 1$, and 2 . These curves are compared with the experimental points. With one exception, all the data taken, namely at sea state 2 (SS2) and 3, for 22 Hz and 45 Hz; at sea state 1/2, 3, and 5 for 32 Hz; and at sea state 2, 3, and 5 for 63 Hz, fit the theoretical curve computed on the basis of omnidirectional surface

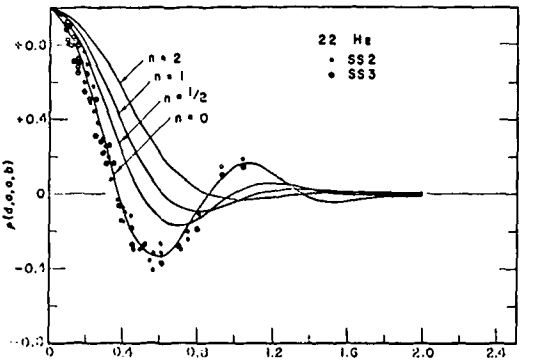

Fig. 41 Experimental values of the spatial correlation compared with the theoretical curves for radiation pattern $\cos^n \alpha$ at 22 Hz and horizontal separation.

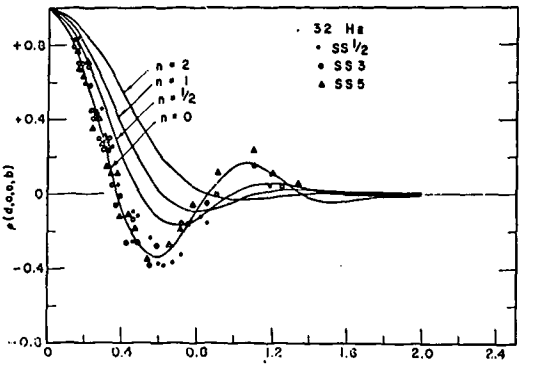

Fig. 42 Experimental values of the spatial correlation compared with the theoretical curves for radiation pattern $\cos^n \alpha$ at 32 Hz and horizontal separation.

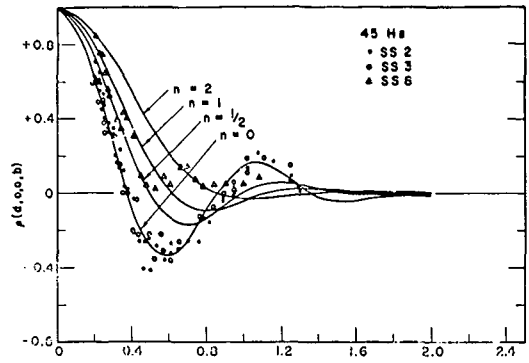

Fig. 43 Experimental values of the spatial correlation compared with the theoretical curves for radiation pattern $\cos^n \alpha$ at 45 Hz and horizontal separation.

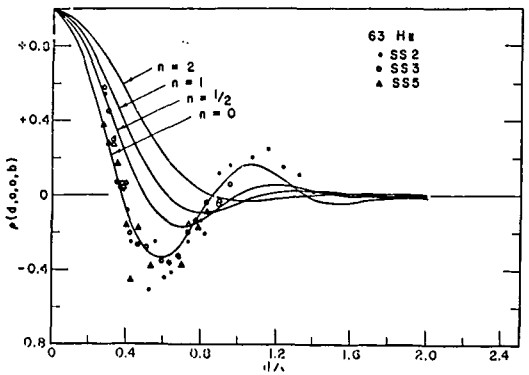

Fig. 44 Experimental values of the spatial correlation compared with the theoretical curves for radiation pattern $\cos^n \alpha$ at 63 Hz and horizontal separation.

sources. However, there is an exception at sea state 8 and 45 Hz; this differs from all of the computed curves. The spatial correlation remained positive and slowly decreased with spacing.

It is pointed out by the Arases[14] that the space-time correlation coefficient for horizontal spacing does not give any significant information of the type of surface sources. From Eq. (3), it is seen that the coefficient is symmetrical with respect to $\tau = 0$ for fixed d, and the principal maximum or minimum is in general located at the origin. The time dependence itself is influenced greatly by the filter characteristics, which are only rough approximations. Figure 45 shows the delay time dependence of the correlation coefficient at 45 Hz spacing of $d/\Lambda = 0.2$ for the various models as compared with the experimental data. Note that the experimental data lies approximately between the omnidirectional curve and the $(\cos \alpha)^{1/2}$ curve.

b. Correlations for Vertically Separated Elements

Spatial and space-time correlations were measured by the Arases with pairs of vertically separated hydrophones at 250, 400, 500, 800, and 1131 Hz. The spatial correlations at these frequencies are shown in Figs. 46 through 50 for sea state 5 at all the above frequencies and at sea state 3 at 400, 800 and 1131 Hz. The sea state 3 data show a greater scatter in the experimental points and are not as reproducible as the sea state 5 data. If the measured results are compared with the theoretical curves computed from Eq. (4) for zero time delay (at 250 Hz and sea state 5), a model of surface radiator with $g(\alpha) = (\cos \alpha)^{1/2}$ appears to fit the data. Here the reproducibility of the correlation coefficients is

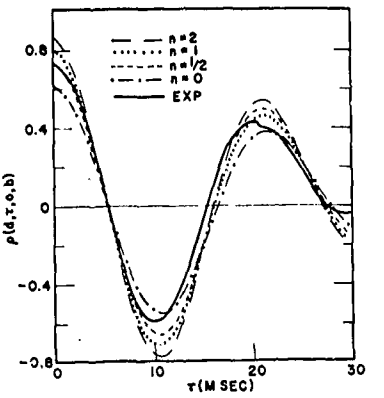

Fig. 45 Experimental and theoretical values of the space-time correlation at 45 Hz and horizontal separation distance $d/\lambda = 0.2$.

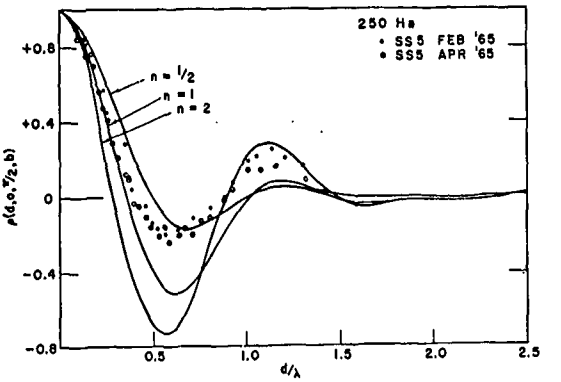

Fig. 46 Experimental values of the spatial correlation compared with the theoretical curves for radiation pattern $\cos^n \alpha$ at 250 Hz and vertical separation.[14]

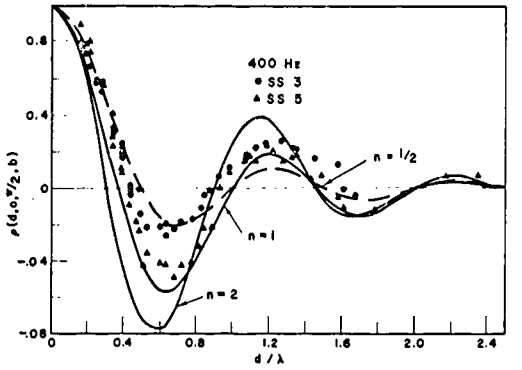

Fig. 47 Experimental values of the spatial correlation compared with the theoretical curves for radiation pattern $\cos^n\alpha$ at 400 Hz and vertical separation.

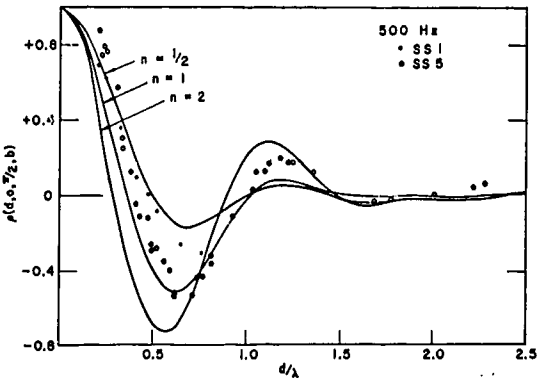

Fig. 48 Experimental values of the spatial correlation compared with the theoretical curves for radiation pattern $\cos^n\alpha$ at 500 Hz and vertical separation.[14]

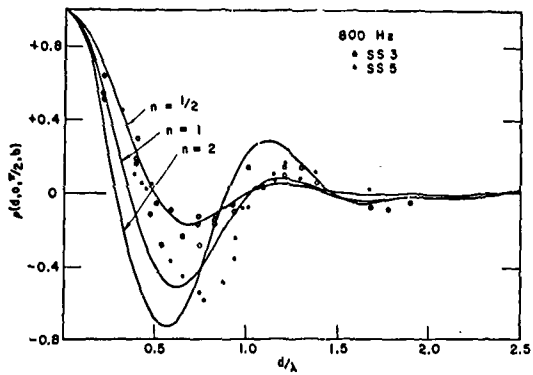

Fig. 49 Experimental values of the spatial correlation compared with the theoretical curves for radiation pattern $\cos^n\alpha$ at 800 Hz and vertical separation.[14]

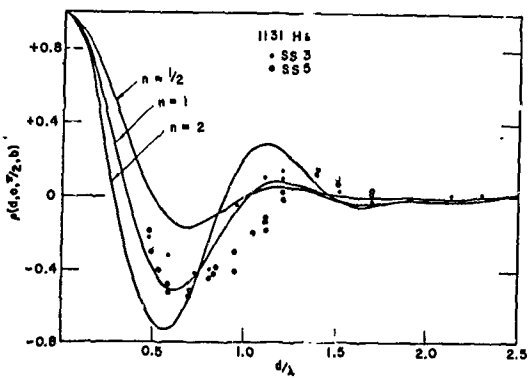

Fig. 50 Experimental values of the spatial correlation compared with the theoretical curves for radiation pattern $\cos^n\alpha$ at 1131 Hz and vertical separation.[14]

shown by the consistency of the data at the same sea state taken several months apart. At sea state 5 and higher frequencies, a uniform distribution of $\cos \alpha$ radiators was found to agree best with the experimental points. It is noted, however, that the measured results show a definite shift with respect to the theoretical curve as the frequency increases. This is illustrated in Fig. 51 on which the best fit curves to the experimental data are given at sea state 5. This shift is explained in part by considering the ambient noise spectrum itself. Typical ambient noise sprectrum curves decrease with frequency in this frequency range. The product of filter response and ambient noise spectrum shifts the center of the response curve to lower frequencies and effectively larger wavelengths; the equivalent d/λ therefore would be smaller.

The 400 Hz and 800 Hz measurements at SS3 seem to indicate a good fit to the $(\cos \alpha)^{1/2}$ computed values. This is questioned by the Arases because the time dependence of the correlation does not confirm the fit.

A typical time correlation at 400 Hz, sea state 3, and separation $d/\lambda = 0.4$ is shown in Fig. 52. Here the agreement with the theoretical curves is qualitative at best. The principal peak of the space-time correlation is in general lower than the theoretically predicted one, and disagreement increases with increasing time delay. The height of the principal maximum is dependent on the filter characteristics; these characteristics were only crudely approximated by the assumption of flat bandwidth. However, the measured autocorrelation of a sample shown by the Arases in Ref. 12 is said to agree well with that computed for a rectangular noise spectrum.

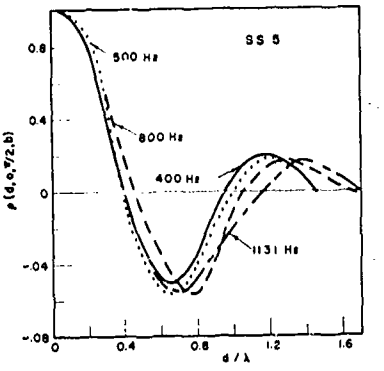

Fig. 51 Best fit to experimental spatial correlation curves at SS5 and vertical spacing at 500-1131 Hz.[14]

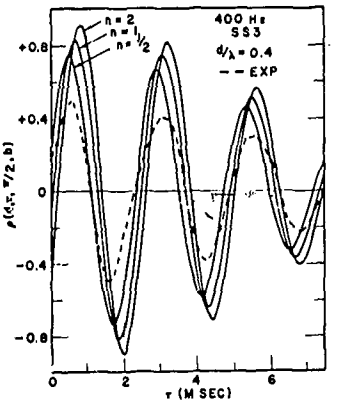

Fig. 52 Experimental and theoretical values of the space-time correlation at 400 Hz and vertical separation distance $d/\lambda = 0.4$.[14]

The delay at which the principal peak of the space-time correlation appears as a function of distance gives some information about possible types of sources. For a radiation pattern of $g(\alpha) = (\cos \alpha)^{1/2}$, the principal maximum occurs at

$$\tau_{max} = (d/2c) \quad \text{for} \quad d < \lambda \ .$$

At and above one wavelength for the $\cos^{1/2}\alpha$ model, two principal maxima occur; this was not observed experimentally. Since at 250 Hz a wavelength is about 20 ft, the data given in Fig. 53 at this frequency may possibly be explained by the $(\cos \alpha)^{1/2}$ model. The data at 500 Hz, shown in the same figure, fit the $\cos \alpha$ theoretical curve well. The same is said to hold true for the results at 400 and 800 Hz, shown in Fig. 54, which was given in a previous paper. At lower sea states the peak of the correlation function does not seem to shift with respect to delay time although its height changes. This may be seen from Fig. 55 which gives the time delay for the principal maximum as a function of separation at sea state 3 and 5 at 1131 Hz.

A summary of the results, by E. M. Arase and T. Arase, for horizontal and vertical correlation measurements is tabulated in Table XV.

One of the most recent papers by E. M. Arase and T. Arase[5] deals with the mapping of the space-time correlation of ambient sea noise. The space-time correlation of ambient noise in the ocean was measured with vertical elements at a depth of 14,500 ft at 800 Hz and sea state 6. The data are presented in the form of a map which shows the principal maximum and zero axis crossings for comparison with recent theoretical work.[46,47]

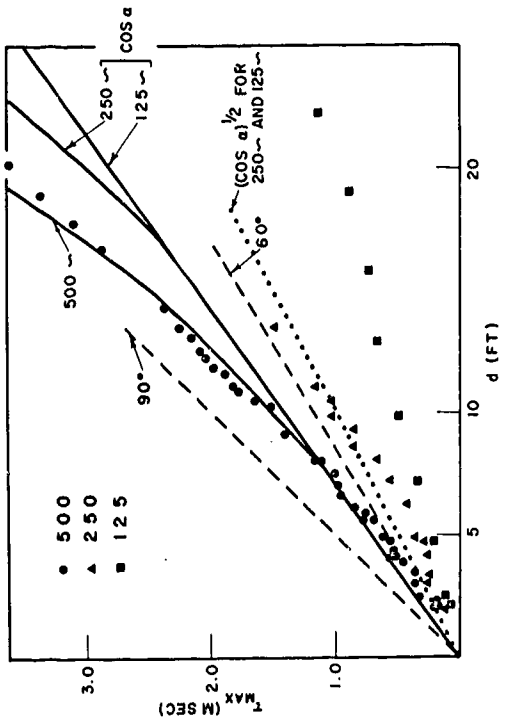

Fig. 53 Time delay corresponding to principal maximum as a function of separation distance and compared with theoretical curves at 125, 250, and 500 Hz.[14]

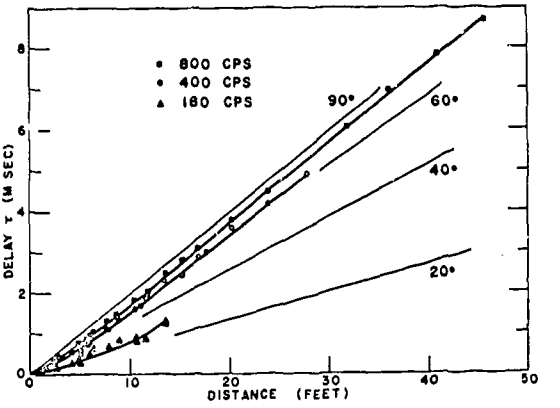

Fig. 54 Time delay as a function of separation distance at 180, 400, 800 Hz.

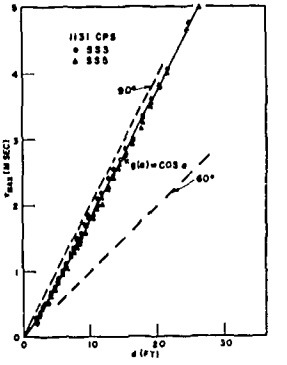

Fig. 55 Time delay corresponding to principal maximum as a function of separation distance at SS3 and 5 for 1131 Hz.[14]

Table XV

Summary of Measured Horizontal and Vertical Correlations for the Arase Model

Hydrophones	Frequency	Sea State	Possible Model
Horizontal Pairs	22-63 Hz range	1/2 to 5	Uniform distribution of omnidirectional surface radiators
Horizontal Pairs	45 Hz	8	One of models fits experimental data
Vertical Pairs	250 Hz	5	$(\cos \alpha)^{1/2}$ model
Vertical Pairs	400 Hz and above	5	Uniform distributions of $\cos \alpha$ radiators give good fit for spatial correlations as well as delay times, at which the principal peaks of the correlation occur
Vertical Pairs	400-1131 Hz	3	No satisfactory fits to theoretical model

Referring to a paper by Liggett and Jacobson[46] the experimental data obtained from directivity measurements with a vertical array are fitted with a directional noise field at the receiver, of the form:

$$N(\theta) = A\, e^{A\cos\theta}/(2\pi e^{A}-1)$$

where θ is the angle from the vertical and A is a parameter that varies according to sea state and frequency. The correlation of ambient noise is then computed from this noise field. In another paper (Lytle and Moose[47]), a uniform distribution of surface dipole noise sources is assumed. This model has been shown to give reasonable agreement with experimental results at 400 Hz and at higher frequencies. However, until the publication of Ref. 5 there were no experimental maps of the space-time correlation. Figures 56, 57, and 58 are experimental maps of the space-time correlation as given in Ref. 5. Figure 56 illustrates a map of the space-time correlation at sea state 6 for vertical elements and 800 Hz, with time delay τ in milliseconds and the element separation d in feet or fraction of the wavelength λ as variables. Experimental points for the zero axis crossings are connected by straight lines. Greater detail from these measurements was not possible because the experimental accuracy decreases with increasing spatial separation and time separation from the principal peak. The time separation is shown explicitly and is reproducible to ± 0.1 msec at all separations. The shaded areas correspond to the negative correlations, the light areas to positive correlations. All of the axis crossings lines show the general tendency and slope of the line connecting the largest correlation peak. At sea state 6 and 800 Hz a

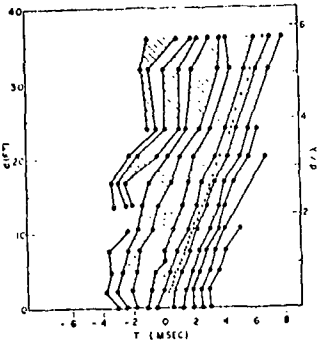

Fig. 56 Experimental map of the space-time correlation of ambient sea noise for vertical elements at 800 Hz, sea state 6. \\\: Negative correlation. ●: Zero. ●: Largest peak.[5]

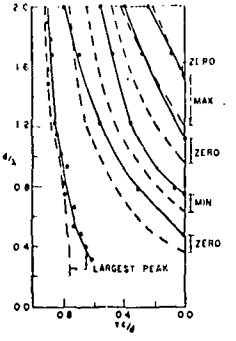

Fig. 57 Map of the experimental and theoretical (Ref. 46) space-time correlation for vertical elements at 800 Hz. ——: Experimental. ---: Liggett.[5]

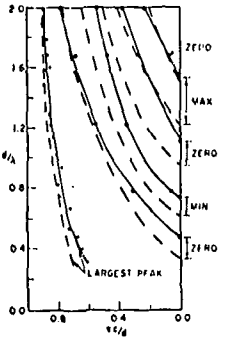

Fig. 58 Map of the experimental and theoretical (dipole surface sources) space-time correlation for vertical elements at 800 Hz. ---: Dipole model. ——: Experimental.[5]

value of $A = 3$ in the equation for $N(\theta)$ seems to fit the directivity data best. Only single frequency maps or those for a bandwidth of approximately 1.6 are given in Ref. 46. However, since the positions of the maxima and zeros for small time delays are not greatly affected by the bandwidth, the experimental results were compared with a bandwidth of 1.25 with those of Ref. 46 with a bandwidth of 1.6 in Fig. 57. The units are dimensionless; where $c = 500$ ft/sec is the velocity of sound. In Fig. 58, the experimental results are compared with the computed results for a dipole model with white noise with a bandwidth of 1.25. From Figs. 57 and 58 it is suggested that the results for both theoretical models are almost identical at small $\tau c/d$. Both of these fit the experimental data qualitatively except at small spacings for the principal maximum and at the location of the first 0 curve.

ACKNOWLEDGMENT

The author gratefully acknowledges permission granted by the authors whose figures have been reproduced in this report.

BIBLIOGRAPHY

1. V. O. Knudsen, R. S. Alford, and J. W. Ewing, "Survey of underwater sound, Report No. 3; Ambient Noise," NDRC SEC., No. 6.1 - NDRC-1848, 1944 (Conf.); "Underwater ambient noise," J. Marine Res. 7, 410 (1948).
2. A. Berman and A. J. Saur, "Ambient noise power spectrum from 1 to 100 cps," 8th Navy Symp. on Underwater Acoustics, New London, (1953).
3. W. C. Beckman, "Low-frequency ambient sea noise," J. Underwater Acoustics (USN) 5, 161 (1955).
4. R. Halley et al., Measurements of Underwater Ambient Noise at Point Sur and Point Arena, California, NEL Report 623 (1955). (Conf.)
5. E. M. Arase and T. Arase, "Mapping of the space time correlation of ambient sea noise," J. Acoust. Soc. Am. 40, 499-500 (1966).
6. F. G. Weigle and A. J. Perrone, Ambient Noise Spectra in the ARTEMIS Receiver Area, U.S.L. Report No. 737 (27 Dec. 1966). (Conf.)
7. T. Arase et al., "Time variability of ambient noise directionality," J. Acoust. Soc. Am. 36, 1015 (1964).
8. T. Arase, E. Arase, F. Weigle, and A. Perrone, Effective Directivity Index of the 1963 Artemis Modules During Winter Conditions (U), Artemis Report No. 33 (June 25, 1964). (Conf.)
9. T. Arase and E. Arase, "Ambient noise measurements with the Artemis modules," Paper J6, Proc. of the 22nd U.S. Navy Symposium on Underwater Acoustics, Oct. 26-28, 1964, pp. 543-547. (Conf.)
10. T. Arase and E. M. Arase, "Spectra and correlations of ambient sea noise at Bermuda," Paper 2C2, Proc. of 23rd Underwater Sound Symposium, Nov. 30-Dec. 2, 1965, pp. 259-267. (Conf.)

11. E. M. Arase and T. Arase, "On the statistics of ambient noise," J. Acoust. Soc. Am. 41, 1597 (A) (1967).

12. T. Arase and E. M. Arase, "Correlation of ambient noise in the ocean," J. Acoust. Soc. Am. 38, 146-148 (1965).

13. E. M. Arase and T. Arase, "Ambient sea-noise correlation," J. Acoust. Soc. Am. 38, 920 (1965).

14. E. Arase and T. Arase, "Correlation of ambient sea noise," J. Acoust. Soc. Am. 40, 205-210 (1966).

15. T. Arase, Directivity of Deep Water Ambient Noise in the Artemis Frequency Range (U), Tech. Memo. A-107 (Dec. 19, 1963). (Conf.)

16. T. Arase and E. M. Arase, "Directivity index of a three-dimensional array of directional sources," J. Acoust. Soc. Am. 35, 735 (1963).

17. E. M. Arase and T. Arase, "Arrays for the measurement of the angular distribution of ambient noise in the ocean," J. Acoust. Soc. Am. 35, 1884 (1963).

18. Pub. No. 700, "Oceanographic Atlas of the North Atlantic Ocean," Section IV, Sea and Swell, U.S. Naval Oceanographic Office, Washington, D.C. (1963).

19. G. M. Wenz, "Acoustic ambient noise in the ocean: Spectra and sources," J. Acoust. Soc. Am. 34, 1936-1956 (1962).

20. G. H. Franz, "Splashes as sources of sound in liquids," J. Acoust. Soc. Am. 31, 1080 (1959).

21. H. M. Fitzpatrick and M. Strasberg, David Taylor Model Basin Report 1269 (January 1959).

22. R. W. Hasse, Draft. 6/1/65, "Artemis Ambient Noise Review," (for Artemis Handbook).

23. Whales and Sharks, Supplement No. 1, Convoy Atlas for the North Atlantic Ocean, HO Publication No. 764 (1954).

24. Charles H. Townsend, The Distribution of Certain Whales as Shown by Logbook Records of American Whaleships, New York Zoological Society, Zoologica, Volume XIX, No. 1 (1960).

25. M. D. Fish, Marine Mammals of the Pacific with Particular Reference to the Production of Underwater Sounds, Woods Hole Oceanographic Institution, Report 49-30 (1944).

26. M. D. Fish, An Outline of Sounds Produced by Fishes in Atlantic Coastal Waters - Sound Measurement and Ecological Notes, Narragansett Marine Laboratory, Special Report No. 1, 53-1 (January 1953).

27. H. M. Walkinshaw, (B.T.L.), Ambient Noise Obtained on 460-Fathoms Site at Bermuda, unpublished B.T.L. Memo (1961). (Conf.)

28. A. D. Little, Report No. 1250862, Survey on Ambient Sea Noise, (August 1962). "Originated by Bolt, Beranek & Newman, Inc. under subcontract to A. D. Little." (Conf.)

29. A. H. Green, Bell Telephone Lab. Tech. Report No. 10 (1962).

30. T. Arase and E. M. Arase, "A review of recent developments in underwater ambient noise," J. Underwater Acoustics (USN) 15, 589-601 (July 1965). (Conf.)

31. E. Arase and T. Arase, "Ambient sea noise in the deep and shallow ocean," J. Acoust. Soc. Am. 42, 73-77 (1967).

32. E. Arase, "On the discrimination factor for a continuous distribution of noise sources," J. Acoust. Soc. Am. 36, 785-786 (1964).

33. C. L. Bretschneider, "Wave forecasting," Ocean Industry (October 1967).

34. R. J. Urick, "Correlative Properties of ambient noise at Bermuda," J. Acoust. Soc. Am. 40, (1966).

35. T. Arase and E. Arase, "Curves of Ambient Noise Spectrum Levels vs. Wind Speed." These sets of curves are not part of any referenced formal or informal document.

36. M. T. Dow, S. W. Emling, and V. O. Knudson, "Survey of underwater sound," Report No. 4, Sounds from Surface Ships; Tech. Report of Division 6, NDRC, No. 2124 (15 June 1945). (Conf.)

37. M. J. Sheely and R. Halley, "Measurement of the attenuation of low frequency underwater sound," J. Acoust. Soc. Am. 29, 464 (1957).

38. F. E. Hale, "Long range propagation in the deep ocean," J. Acoust. Soc. Am. 33, 456 (1961).

39. P. G. Cable, Interference in an ARTEMIS System Due to Radiated Shipping Noise, U.S.L. Tech. Memo. No. 905-053-61 (26 May 1961). (Conf.)

40. C. R. Rumpel, "Density of ships in the North Atlantic." (26 October 1964) (U), in Advance Defense System, Second Interim Report, B.T.L. Report No. OBJ-7829 X-2 (4 December 1964). (Secret)

41. W. H. Thorp, "Deep-sea ocean sound attenuation in the sub and low kilocycle-per-second region," J. Acoust. Soc. Am. 4, 648-654 (1965).

42. V. M. Albers, Underwater Acoustics Handbook - II, Penn. State Univ. Press (1965).

43. M. P. Fish, Biological Sources of Sustained Ambient Sea Noise, Narragansett Marine Laboratory Tech. Report No. 19 (March 1964).

44. J. Edie, Space Time Correlation Functio. .f Surface Generated Noise, Litton Systems, Inc., Waltham, Mass., Rept. TR63-9-BF, Contract Nonr 3320(00) (1963).

45. W. S. Liggett and M. J. Jacobson, "Covariance of noise in attenuating media," J. Acoust. Soc. Am. 36, 1183-1194 (1964).

46. W. S. Liggett and M. J. Jacobson, "Noise covariance and vertical directivity in deep ocean," J. Acoust. Soc. Am. 39, 280-288 (1966).

47. D. W. Lytle and P. H. Moose, "Space-time correlation functions for surface-noise model," J. Acoust. Soc. Am. 39, 487-590 (1966).

48. C. Nicholas Pryor, Some Effects of Inter-Element Correlation and Clipping on the Performance of Receiving Arrays (September 1966), NOLTR G6-53, U.S. Naval Ordnance Laboratory, White Oak, Maryland.

49. B. F. Cron and C. H. Sherman, "Spatial-correlation functions for various noise fields," JACSA, 1732 (Nov. 1962).

50. B. F. Cron and C. H. Sherman, "Spatial correlation functions for various noise models," J. Acoust. Soc. Am. 38, 885 (1965).

51. R. J. Talham, "Ambient-sea noise model," J. Acoust. Soc. Am. 36, 1541-1544 (1964).

52. B. F. Cron, B. C. Hasse, and F. J. Keltonic, "Comparison of theoretical and experimental values of spatial correlation," J. Acoust. Soc. Am. 37, 523-529 (1965).

53. D. F. Morrison, Some Statistic Information on Natural Background, Sea Noise on the Portland and Bexington Noise Ranges, Admiralty Underwater Weapons Establishment, Portland, England, (Nov. 1964). (Conf.)

54. A. W. Ellinthorpe, Notes on Undersea Acoustic Communications, U.S.L. Report No. 826, (May 1967). (Conf.)

Additional Bibliography not Referenced

in Text and Appendix

55. S. M. Levin, "The SST - How Good?," Space/Aeronautics, p. 87 (July 1967).

56. D. Maglieri, "Source effects of airplane operations and the atmosphere on sonic-boom signatures," J. Acoust. Soc. Am. 39, part 2, S36-S42 (May 1966).

57. H. Hubbard, "Nature of the sonic boom problem," J. Acoust. Soc. Am. 39, part 2, S3 (May 1966).

58. D. G. Tucker and B. K. Garey, Applied Underwater Acoustics, Pergammon Press, Ltd., London (1966).

59. R. W. Young, "Underwater ambient noise, a review," U.S. NEL, California, Paper No. 2C1, 23rd Symposium on Underwater Acoustics, 1965. (Conf.)

60. Axelrod et al., (A. D. Little and USNSL), "Vertical directionality of ambient noise in the deep ocean at a site near Bermuda," J. Acoust. Soc. Am. 37, 77-83 (1965).

61. "Project AUTEC systems analysis study," Vol. 4, Environmental Factors, Lockheed Aircraft Co. (August 1961). (Conf.) (See Ref. 28.)

62. W. B. McAdams and R. I. Tait, "Ambient sea noise off the New Zealand Coast," J. Underwater Acoustics (USN) 11, 653 (1961). (See Ref. 28.)

63. G. M. Wenz and C. Castien, Underwater Ambient Noise Measurements in the Bering Straits off Wales, Alaska, NEL Report 889 (1959). (Conf.) (See Ref. 28.)

64. Project Jezebel Progress Reports, ONR Contract Nonr-210(00) B. T. L. (1951-1954). (Secret)

65. D. Ross, Data for the Underwater Data Systems Dept., B.T.L. (1958). (Conf.) (See Ref. 28.)

66. J. D. Richard, Jr., Underwater Ambient Noise in the Straits of Florida and Approaches, Miami U. Marine Lab., Report 56-12 (1956). (Conf.) (See Ref. 28.)

67. T. E. Heindsmann, et al., "Effect of rain on underwater noise levels," J. Acoust. Soc. Am. 27, 378 (1955).

68. G. M. Wenz, H. M. Linnette, and C. N. Miller, Underwater Ambient Noise Measurements in the North Central Pacific, Chinook Expedition, NEL Report 855 (July 18, 1958).

69. E. Rhian, Acoustic Ambient Noise in the Tongue of the Ocean, Univ. of Miami Report (July 1959). (Conf.)

70. B. C. Hassel and F. J. Keltonic, The Effect of Wind Speed on Spatial Correlation of Ambient Noise, U.S. Navy Underwater Sound Lab. Report No. 596 (9 May 1966).

71. Julian Stone, "Problems associated with measurement of ambient-noise directivity by means of linear additive arrays," J. Acoust. Soc. Am. 34, 328-333 (1962).

72. W. S. Liggett and M. J. Jacobson, "Covariance of surface-generated noise in a deep ocean," J. Acoust. Soc. Am. 38, 303 (1965).

73. D. Middleton, "Detection of random acoustic signals by receivers with distributed elements," J. Acoust Soc. Am. 38, 727 (1965).

74. D. W. Little, "Space time correlation functions for surface-noise model," J. Acoust. Soc. Am. 39, 587 (1966).

75. H. M. Linnette and R. J. Thompson, "Directivity study of the noise field in the ocean, employing a correlative dipole," J. Acoust. Soc. Am. 36, 1788 (1964).

76. E. H. Axelrod, B. H. Schooner, and W. A. Von Winkle, "Vertical directionality of ambient noise in the deep ocean at a site near Bermuda," J. Acoust. Soc. Am. 37, 77 (1965).

77. G. R. Fox, "Ambient-noise directivity measurements," J. Acoust. Soc. Am. 36, 1537 (1964).

78. A. Berman, "Spatial correlation of ambient noise," J. Acoust. Soc. Am. 32, 920 (A) (1960).

79. F. Weigle, Acoustic Propagation Measurements with the USS MALOY in February 1962, U.S.L. Tech. Memo. No. 906-02-62, (17 Dec. 1962). (Conf.)

80. M. Strasberg, "Gas bubbles as sources of sound in liquids," J. Acoust. Soc. Am. 28, 20 (1956).

81. M. A. Calderson, Probability Density Analysis of Ocean Ambient and Ship Noise, USNEL Report No. 1248 (5 Nov. 1964).

82. W. N. Tavolga, Ed., "Marine Bio-Acoustics." Proceedings of a Symposium held at Lerner Marine Laboratory, Bimini, Bahamas, April 1963, Pergammon Press (1964).

83. C. Nixon and P. Borsky, "Effects of sonic boom on people: St. Louis, Mo., 1961-1962," J. Acoust. Soc. Am. 35, part 2, S51 (1966).

84. H. Carlson, R. Mack, O. Morris, "Sonic-boom pressure-field estimation techniques," J. Acoust. Soc. Am. 39, part 2, S10-S18 (1966).

85. H. Von Gierke, "Effects of sonic-boom on people: Review and outlook," J. Acoust. Soc. Am. 39, part 2, S43-S50 (1960).

86. I. Tolstoy and C. S. Clay, Ocean Acoustics, McGraw-Hill Book Co., New York (1966).

87. Blair Kirsman, Wind Waves, Prentice-Hall, New York (1965).

88. W. J. Pierson and L. Moskowitz, "A proposed spectral form for fully developed wind seas based on the similarity theory of S. A. Kitarigorodski," J. Geophys. Res. 69, 5181-5190 (1964).

89. V. Cornish, Ocean Waves, University Press, Cambridge, Mass. (1934).

90. W. J. Pierson et al., Observing and Forecasting Ocean Waves by Means of Wave Spectra and Statistics, Hydrographic Office Publication No. 603, U.S. Dept. of the Navy (1955).

APPENDIX A

Wind-Speed Distributions From Oceanographic Atlas[18]

February Through December at 33° N, 67° W

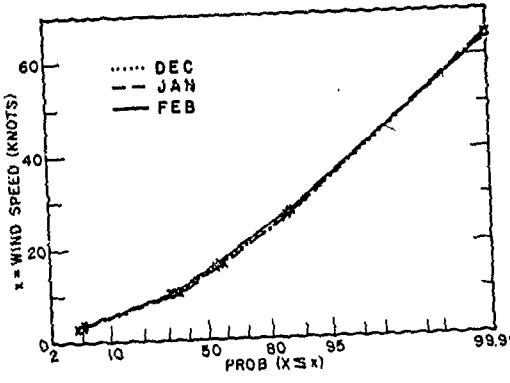

Fig. A-1 Wind speed distribution from Atlas[18] for December, January, and February.

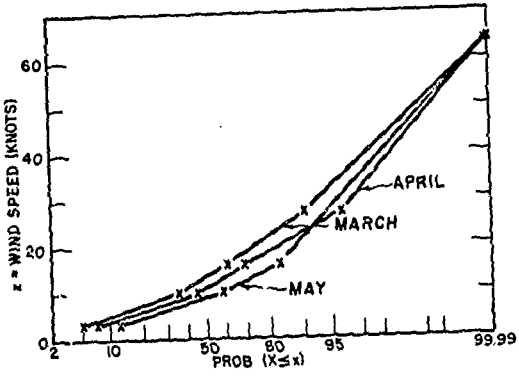

Fig. A-2 Wind speed distribution from Atlas[18] for March, April, and May.

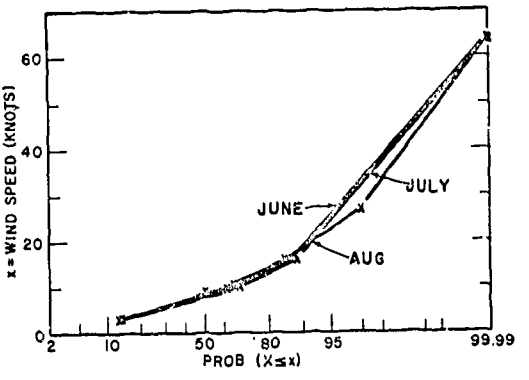

Fig. A-3 Wind speed distribution from Atlas[18] for June, July, and August.

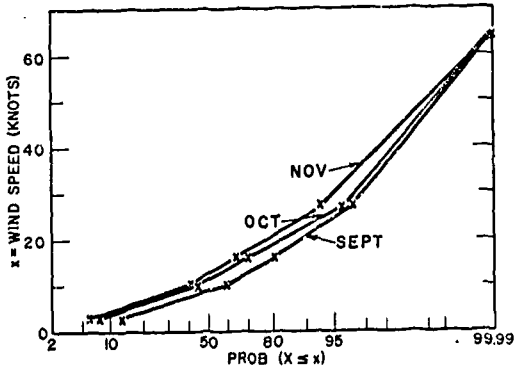

Fig. A-4 Wind speed distribution from Atlas[18] for September, October, and November.

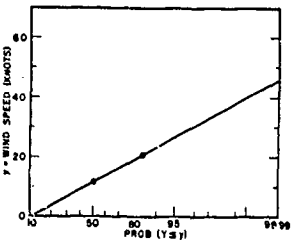

Fig. A-5 Wind speed distribution curve constructed from average mean and standard deviation. January through December, 33° N, 67° W.[18]

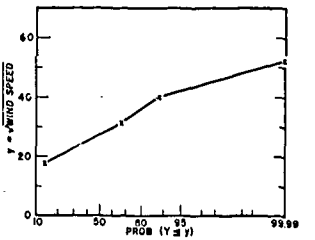

Fig. A-6 Wind speed distribution plotted as square root speed (July). 33° N, 67° W, 2544 samples.[18]

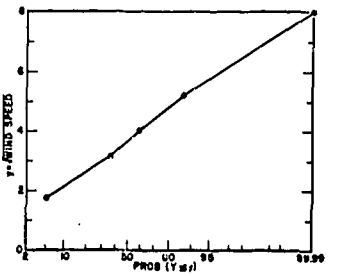

Fig. A-7 Wind speed distribution plotted as square root of wind speed (January), 33° N, 67° W, 2660 samples.

APPENDIX B

Comparison of Artemis Noise Data with Data From Other Areas

Table B-I

Comparison of Arase and Wenz Data[9,19]

knots	Figure 5: 400 Hz Spectrum levels vs. wind speed Winter knots	Winter dB/1 μbar	Summer knots	Summer dB/1 μbar	Figure 6: Regression lines of 400 Hz Spectrum levels vs. wind speed Jan dB	Feb dB	Apr dB	May dB	Aug dB	Dec dB
2	2	-37	-	-	-	-45	-	-	-	-52
5	5	-37	-	-	-	-37	-	-40	-42	-43
10	10	-34	10	-37	-38	-33	-33	-38	-37	-38
20	20	-28	20	-34	-34	-28	-26	-36	-	-32
30	30	-25	30	-30	-	-	-	-	-	-
40	40	-22	-	-	-	-	-	-	-	-
50					-	-20	-	-	-	-24

Wind Force (Beaufort)	Summer (Fig. 9). dB//1 μbar/Hz Arase 200 Hz	Arase 500 Hz	Arase 1000 Hz	Arase 2000 Hz	Wenz 200 Hz	Wenz 500 Hz	Wenz 1000 Hz	Wenz 2000 Hz
1	-	-	-	-	-56	-54	-55	-60
2	-	-	-	-	-47	-45	-45	-51
3	-33	-37	-41	-	-42	-40	-40	-47
4	-	-	-	-	-	-	-	-
5	-32	-34	-35	-	-34	-32	-35	-41
6	-31	-31	-33	-	-	-	-	-
7	-	-	-	-	-	-	-	-
8	-	-	-	-	-30	-27	-30	-34

Wind Force (Beaufort)	Winter (Fig. 10). dB//1 μbar/Hz Arase 200 Hz	Arase 500 Hz	Arase 1000 Hz	Arase 2000 Hz	Wenz 200 Hz	Wenz 500 Hz	Wenz 1000 Hz	Wenz 2000 Hz
1	-	-40	-47	-	-56	-54	-56	-60
2	-	-38	-45	-	-47	-45	-46	-52
3	-	-35	-41	-	-43	-41	-44	-48
4	-	-	-	-	-	-	-	-
5	-	-29	-33	-	-34	-33	-46	-42
6	-	-	-	-	-	-	-	-
7	-	-	-	-	-	-	-	-
8	-	-22	-23	-	-30	-28	-31	-35

Table B-II

Measured Ambient Noise Levels and Corresponding

Wind Speed, Sea-State and Beaufort Force Numbers

Beaufort Force No.	Sea State	Wind Speed (knots)	Mean Knots	Arase dB//1 µbar for 400 Hz	Wenz dB//1 µbar for 400 Hz
8	7	34-40	37	-28	-30
7	6	28-33	30 1/2	-29	-
6	5	22-27	24 1/2	-31.5	-
5	4	17-21	19	-34	-33
4	3	11-16	13 1/2	-36	-35
3	2	7-10	8 1/2	-39	-37
2	1	4-6	5	-41	-40
1	1/2	1-3	2	-44	-44

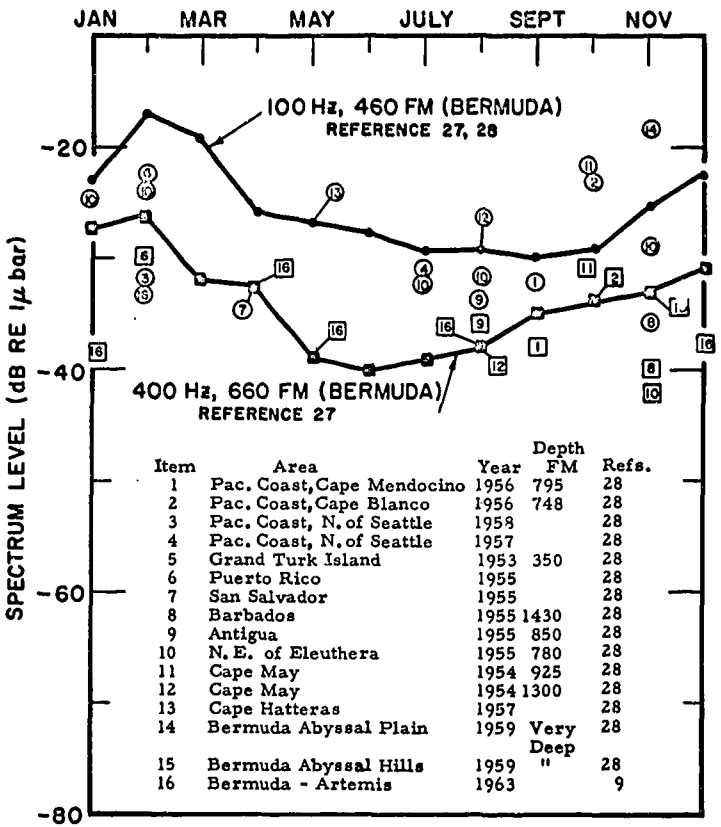

Item	Area	Year	Depth FM	Refs.
1	Pac. Coast, Cape Mendocino	1956	795	28
2	Pac. Coast, Cape Blanco	1956	748	28
3	Pac. Coast, N. of Seattle	1958		28
4	Pac. Coast, N. of Seattle	1957		28
5	Grand Turk Island	1953	350	28
6	Puerto Rico	1955		28
7	San Salvador	1955		28
8	Barbados	1955	1430	28
9	Antigua	1955	850	28
10	N. E. of Eleuthera	1955	780	28
11	Cape May	1954	925	28
12	Cape May	1954	1300	28
13	Cape Hatteras	1957		28
14	Bermuda Abyssal Plain	1959	Very Deep	28
15	Bermuda Abyssal Hills	1959	"	28
16	Bermuda - Artemis	1963		9

Fig. B-1 Monthly variations of ambient noise near Bermuda and other areas.

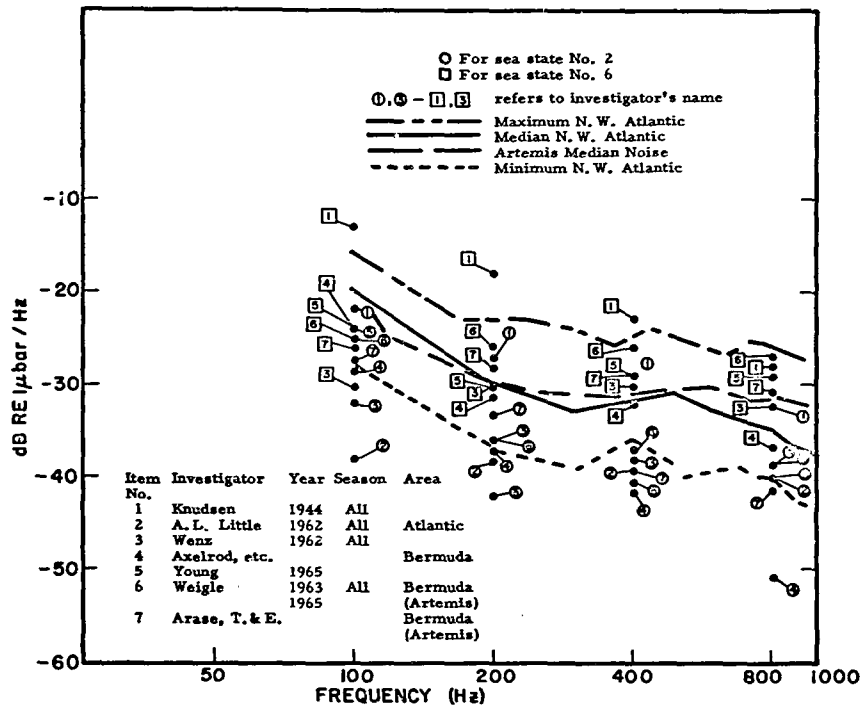

Fig. B-2 Noise levels vs. frequency in Bermuda, Atlantic areas.[9,19]

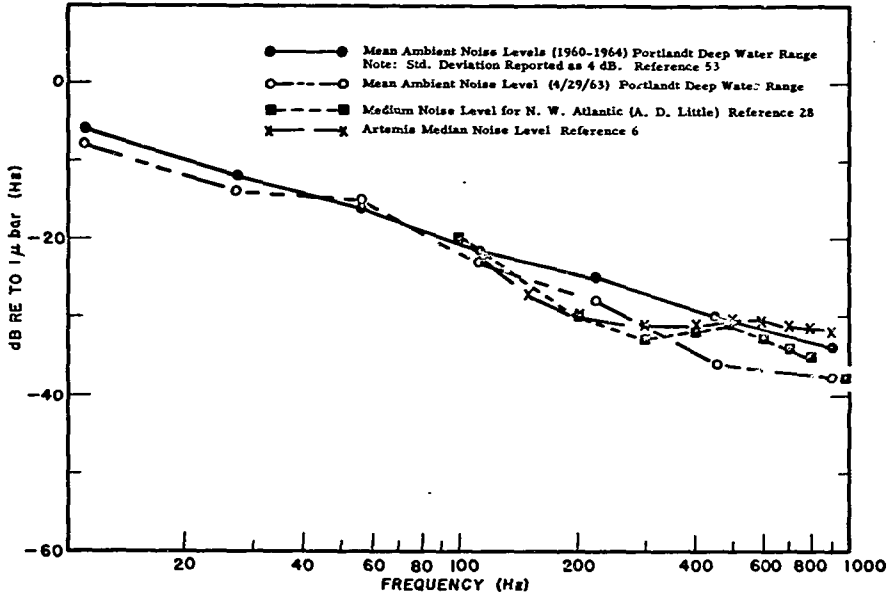

Fig. B-3 Comparison curves of Artemis and Morrison noise data.[9,53]

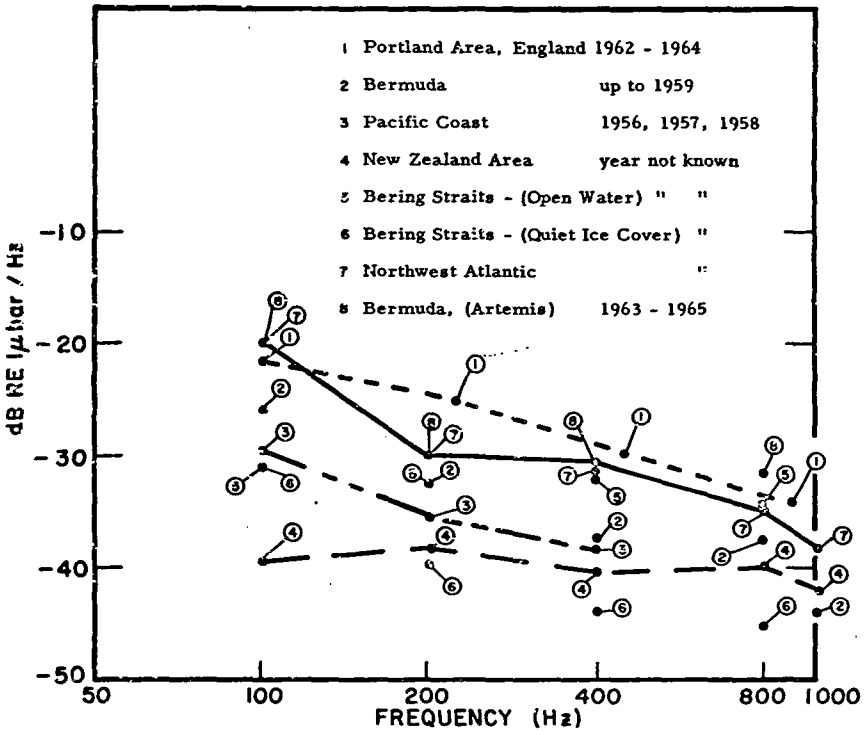

Fig. B-4 Comparison of noise data for various world areas.[9, 19, 53]

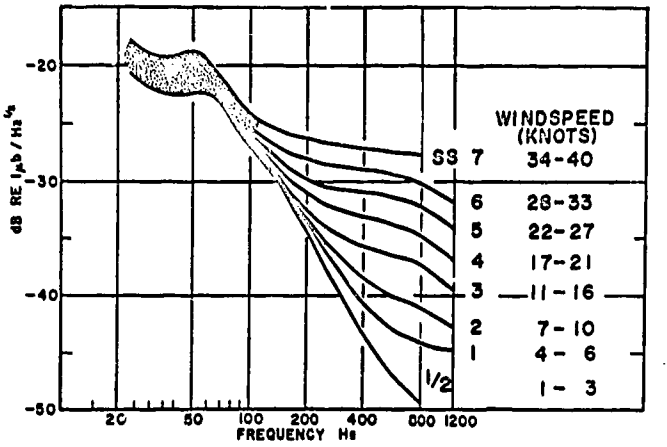

Fig. B-5 Noise spectrum level vs. frequency, wind speed, and sea state.

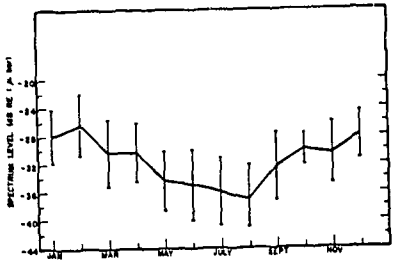

Fig. B-6 Monthly ambient spectrum noise level for 446.4 Hz.[22]

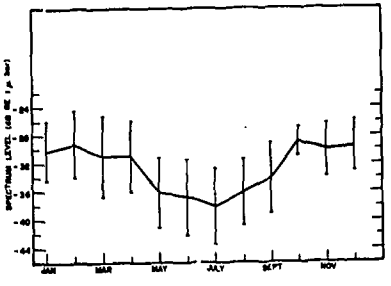

Fig. B-7 Monthly ambient spectrum noise level at 891.1 Hz.[22]

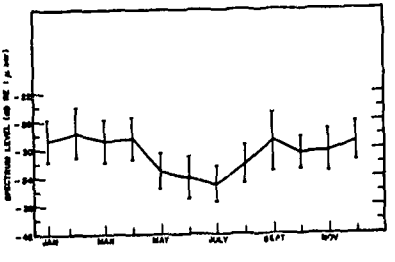

Fig. B-8 Monthly ambient spectrum noise level at 274.7 Hz.[22]

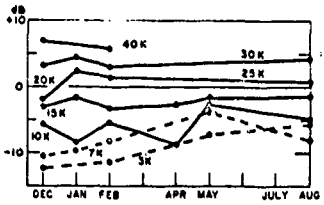

Fig. B-9 400 Hz spectrum level measured during the year normalized to 20 knot noise level; wind speed is the parameter.[9]

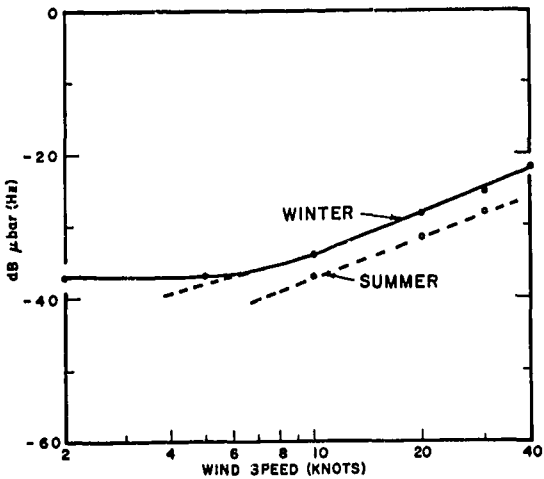

Fig. B-10 400 Hz spectrum level vs. wind speed during winter and summer.[9]

APPENDIX C

Excerpts and Data from D. F. Morrison's Report[53]
on Noise Data Obtained from the Portland and
Bexington Underwater Test Ranges (England)

Systematic record compiled for last four years (1960-1964). Noise spectrum levels measured regularly in each of 16 octaves from 1 Hz to 76 kHz.

Low-Frequency Hydrophone Unit: covered 1 Hz to 200 Hz in 10 octaves.

High-Frequency Hydrophone Unit: covered 75 Hz to 75 kHz in 10 octaves.

Deep Range: Noise levels approached symmetrical distribution in higher low-frequency octaves and most of high-frequency octaves, except for tendency to "tail" into the low noise levels. No explanation for skewness. Octaves most affected by shipping interference are the lowest low-frequency octaves (1 to 8 Hz); also lowest low-frequency octaves most susceptible to long-range interference. (C)

Standard Deviation of Noise: 6 to 8 dB in 1 to 8 Hz band; 4 dB over rest of bands. (C)

Coastal Range: On the average about 3 dB quieter than deep range in the lowest octaves. Coastal range more susceptible to noise due to waves breaking on shore. (C)

Shipping Noise Screened Out: Background noise measurements not taken when shipping was known to be interfering: Variation in noise levels in one day during "quiet" weather is much less than the long-term variation. (C)

Results from the three noise ranges referred to Knudsen curves: for sea state 3 falls -13 dB//1 μbar at 50 Hz to -56 dB//1 μbar at 15 kHz. (C)

Portland Deep Range: (Fig. C-1) Taking noise level in an octave to be that at the center frequency - the mean noise curves for all sea states, referred to Knudsen sea state 3 curve, are within 2 dB over the above frequency range and coincide for large portions of it. (C)

Coastal Range: (Fig. C-2) Gives similar characteristic or average of 3 dB quieter, corresponding to Knudsen sea state 2-1/2. This is in keeping with the partially sheltered position. (C)

Bexington Range: Mean spectrum level for observed sea state 3 is, however, more nearly correspondent with the Knudsen sea state 4 curve. Higher mean level probably due to noise of surf on the Chesil Beach. (C)

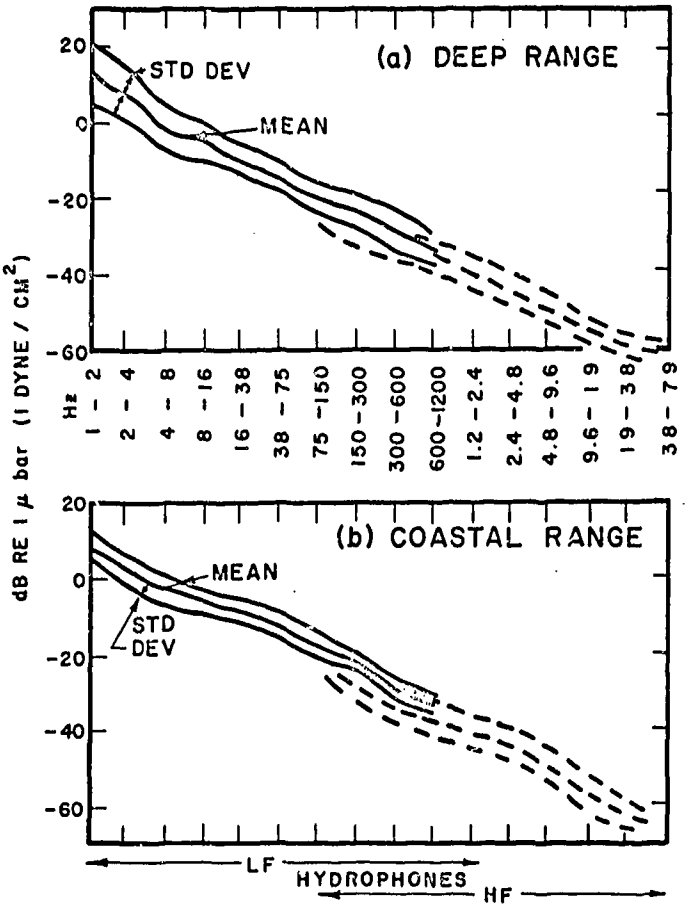

Fig. C-1 Background sea noise 1962-1964.[53]

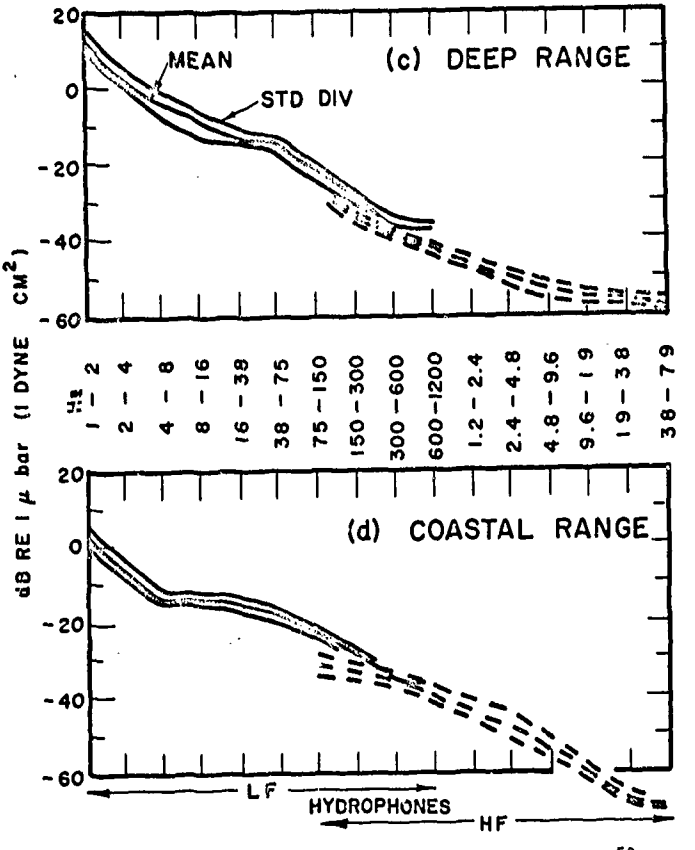

Fig. C-2 Background sea noise in one day SS0 to SS1.[53]

APPENDIX D

Wind-Wave Generation

A. W. Ellinthorpe[54] indicates that there does not exist a complete theory of wind waves for a number of very good reasons. The process of wind-wave generation is non-linear and even in the steady state, non-linear effects are present (such as white caps). The waves interact in complex fashion with the wind, which is in itself a complicated function of space and time. These waves propagate with little loss over great distances and undergo lossy reflections from shores. Statistical descriptions must be used but the process is non-stationary in time and variable in space. Results obtained in water shallower than several wavelengths are affected by a drag force imposed by the bottom; the wavelengths of interest are in the range of several hundreds of feet; so the expression "shallow" in this context is about 1,000 ft. Results obtained from a ship are affected by the motion of the ship.

Figure D-1 is a plot of a widely accepted theoretical power spectrum for wind waves. The normalized form of this curve is due to Bretschneider;[33] the wind-speed relationship is due to Pierson.[90] This is a scalar or one-dimensional spectrum which would be obtained by the rise and fall of water along a pole thrust through the surface. The corresponding vector or two-dimensional spectrum would be a three-dimensional plot which included arrival angles; there does not exist any precise vector spectra. There is a fairly good agreement between the spectrum of Figure D-1 and empirical results. There are also empirical data which indicate that at least the first order statistics, that is the distribution function, are Gaussian.

To round out this picture of the ocean surface and for subsequent reference, Figure D-2 is shown as a plot of the rms amplitude (σ), of the surface waves. The curves of Figure D-2 are a calculation of what would be found if the waves were observed through a rectangular high-pass filter whose cutoff point in wavelengths is plotted as the abscissa. The wind speed is also included as a parameter, and the wavelength corresponding to the frequency at which the spectrum peaks (see Figure D-1) is included as a matter of interest. Note that at a 2-knot wind there is no surface wave energy at wavelengths longer than about 5 ft and the total rms amplitude is about 0.028 ft; at 10 knots the cutoff wavelength is about 120 ft and σ is 0.7 ft. Since the acoustic wavelengths of interest here range upward from 1 ft the inference of surface wave interactions at moderate wind speeds should be obvious.

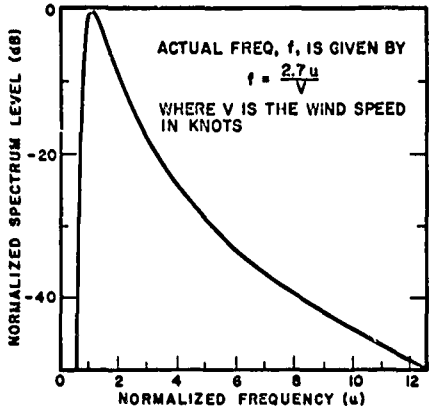

Fig. D-1 A one-dimensional wind wave spectrum.[33]

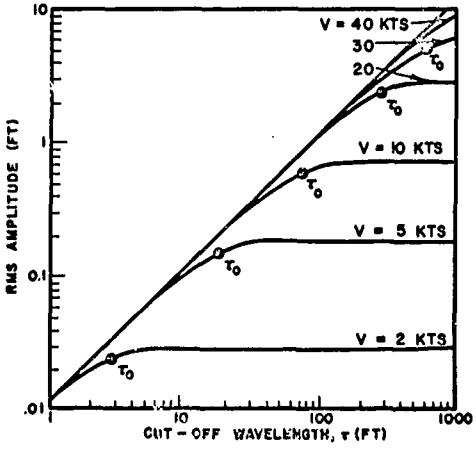

Fig. D-2 Wind wave amplitude as a cumulative function of wave length.[33]

UNCLASSIFIED
Security Classification

DOCUMENT CONTROL DATA - R & D
(Security classification of title, body of abstract and indexing annotation must be entered when the overall report is classified)

1. ORIGINATING ACTIVITY (Corporate author) Hudson Laboratories of Columbia University 145 Palisade Street Dobbs Ferry, New York 10522	2a. REPORT SECURITY CLASSIFICATION CONFIDENTIAL 2b. GROUP 4

3. REPORT TITLE

DEEP OCEAN AMBIENT NOISE

4. DESCRIPTIVE NOTES (Type of report and inclusive dates)

Technical Report

5. AUTHOR(S) (First name, middle initial, last name)

Arthur A. Barrios

6. REPORT DATE	7a. TOTAL NO. OF PAGES	7b. NO. OF REFS
December 1967	156	90

8a. CONTRACT OR GRANT NO.	9a. ORIGINATOR'S REPORT NUMBER(S)
Nonr-266(66) b. PROJECT NO.	ARTEMIS Report No. 64
c. d.	9b. OTHER REPORT NO(S) (Any other numbers that may be assigned this report)

10. DISTRIBUTION STATEMENT

In addition to security requirements which apply to this document and must be met, each transmittal outside the Department of Defense must have prior approval of the Office of Naval Research, Code 480.

11. SUPPLEMENTARY NOTES	12. SPONSORING MILITARY ACTIVITY
	Office of Naval Research, Code 480.

13. ABSTRACT

The objective of this report is to provide information on deep ocean ambient noise which can be used in sonar system design and analysis. Guidelines are given for estimating wind-generated noise, oceanic ship traffic noise, biological noise levels, and the composite ambient noise background. The report also discusses recent measurements and studies on the directional properties of noise, and on the space-time correlations.

Early and recent reports on ambient ocean noise are reviewed and evaluated. Some conclusions are drawn on the variability of reported noise levels in the northwest Atlantic area and on the correlation of wind speed with respect to noise.

DD FORM 1 NOV 65 1473 (PAGE 1)
S/N 0101-807-6811

UNCLASSIFIED
Security Classification
A-31408

14 KEY WORDS	LINK A		LINK B		LINK C	
	ROLE	WT	ROLE	WT	ROLE	WT
Compilation of ambient noise						
Reference for sonar system design						

Hudson Labs., Columbia Univ., Dobbs Ferry, N.Y. DEEP OCEAN AMBIENT NOISE (U), by Arthur A. Barrios. December, 1967. 156 p. (ARTEMIS rept. no. 64.)
(Contract Nonr-266(66)) Confidential report

The objective of this report is to provide information on deep ocean ambient noise which can be used in sonar system design and analysis. Guidelines are given for estimating wind-generated noise, oceanic ship traffic noise, biological noise levels, and the composite ambient noise background. The report also discusses recent measurements and studies on the directional properties of noise, and on the space-time correlations.

Early and recent reports on ambient ocean noise are reviewed and evaluated. Some conclusions are drawn on the variability of reported noise levels in the northwest Atlantic area and on the correlation of wind speed with respect to noise.

1. Underwater sound - Ambient noise
2. Sonar systems - Design - Acoustic factors

I. Title: ARTEMIS
II. Barrios, Arthur A.
III. Contract Nonr-266(66)

Hudson Labs., Columbia Univ., Dobbs Ferry, N.Y. DEEP OCEAN AMBIENT NOISE (U), by Arthur A. Barrios. December, 1967. 156 p. (ARTEMIS rept. no. 64.)
(Contract Nonr-266(66)) Confidential report

The objective of this report is to provide information on deep ocean ambient noise which can be used in sonar system design and analysis. Guidelines are given for estimating wind-generated noise, oceanic ship traffic noise, biological noise levels, and the composite ambient noise background. The report also discusses recent measurements and studies on the directional properties of noise, and on the space-time correlations.

Early and recent reports on ambient ocean noise are reviewed and evaluated. Some conclusions are drawn on the variability of reported noise levels in the northwest Atlantic area and on the correlation of wind speed with respect to noise.

1. Underwater sound - Ambient noise
2. Sonar systems - Design - Acoustic factors

I. Title: ARTEMIS
II. Barrios, Arthur A.
III. Contract Nonr-266(66)

Hudson Labs., Columbia Univ., Dobbs Ferry, N.Y. DEEP OCEAN AMBIENT NOISE (U), by Arthur A. Barrios. December, 1967. 156 p. (ARTEMIS rept. no. 64.)
(Contract Nonr-266(66)) Confidential report

The objective of this report is to provide information on deep ocean ambient noise which can be used in sonar system design and analysis. Guidelines are given for estimating wind-generated noise, oceanic ship traffic noise, biological noise levels, and the composite ambient noise background. The report also discusses recent measurements and studies on the directional properties of noise, and on the space-time correlations.

Early and recent reports on ambient ocean noise are reviewed and evaluated. Some conclusions are drawn on the variability of reported noise levels in the northwest Atlantic area and on the correlation of wind speed with respect to noise.

1. Underwater sound - Ambient noise
2. Sonar systems - Design - Acoustic factors

I. Title: ARTEMIS
II. Barrios, Arthur A.
III. Contract Non--266(66)

Hudson Labs., Columbia Univ., Dobbs Ferry, N.Y. DEEP OCEAN AMBIENT NOISE (U), by Arthur A. Barrios. December, 1967. 156 p. (ARTEMIS rept. no. 64.)
(Contract Nonr-266(66)) Confidential report

The objective of this report is to provide information on deep ocean ambient noise which can be used in sonar system design and analysis. Guidelines are given for estimating wind-generated noise, oceanic ship traffic noise, biological noise levels, and the composite ambient noise background. The report also discusses recent measurements and studies on the directional properties of noise, and on the space-time correlations.

Early and recent reports on ambient ocean noise are reviewed and evaluated. Some conclusions are drawn on the variability of reported noise levels in the northwest Atlantic area and on the correlation of wind speed with respect to noise.

1. Underwater sound - Ambient noise
2. Sonar systems - Design - Acoustic factors

I. Title: ARTEMIS
II. Barrios, Arthur A.
III. Contract Nonr-266(66)

DEPARTMENT OF THE NAVY
OFFICE OF NAVAL RESEARCH
800 NORTH QUINCY STREET
ARLINGTON, VA 22217-5660

IN REPLY REFER TO
5510/1
Ser 43/326
19 Apr 00

From: Chief of Naval Research
To: Defense Technical Information Center
(DTIC-OCQ)
8725 John J Kingman Road Suite 0944
Ft. Belvoir VA 22060-6218

Subj: CLASSIFICATION CHANGE

Ref: (a) AD # 394 475 (ARTEMIS Report No. 64, Deep Ocean Ambient Noise)

1. Reference (a) has been downgraded to UNCLASSIFIED by authority of the Chief of Naval Research, 19 April 2000. Distribution Statement A should be assigned to the document.

2. Questions may be directed to the undersigned on (703) 696-4619.

Peggy Lambert

PEGGY LAMBERT
By direction

Completed 5-12-00

Received 4-28-00